EUROPEAN FUSION DEVELOPMENT AGREEMENT

EFDA–JET–PR(04)50

J.P. Coad, J. Likonen, M. Rubel, E. Vainonen-Ahlgren,
D.E. Hole, T. Sajavaara, T. Renvall, G. F. Matthews
and JET EFDA Contributors

Overview of Material Re-deposition and Fuel Retention Studies at JET with the Gas Box Divertor

Overview of Material Re-deposition and Fuel Retention Studies at JET with the Gas Box Divertor

J.P. Coad[1], J. Likonen[2], M. Rubel[3], E. Vainonen-Ahlgren[1], D.E. Hole[4], T. Sajavaara[5], T. Renvall[2], G. F. Matthews[1]
and JET EFDA Contributors*

[1]*Culham Science Centre, Association EURATOM – UKAEA-Fusion, Abingdon, Oxfordshire, OX14 3DB, United Kingdom*
[2]*Association EURATOM-TEKES, VTT Processes, P.O. Box 1608, 02044 VTT, Espoo, Finland*
[3]*Alfvén Laboratory, Royal Institute of Technology, Association EURATOM – VR, 100 44 Stockholm, Sweden*
[4]*School of Mathematical and Physical Sciences, Accelerator Laboratory, University of Sussex, BN1 9QH Brighton, United Kingdom*
[5]*Accelerator Laboratory, University of Helsinki, P.O. Box 43, 00014 University of Helsinki,*
** See annex of J. Pamela et al, "Overview of Recent JET Results and Future Perspectives", Fusion Energy 2002 (Proc.19 th IAEA Fusion Energy Conference, Lyon (2002)).*

Preprint of Paper to be submitted for publication in
Nuclear Fusion

ABSTRACT

In the period 1998 – 2001 the JET tokamak was operated with the Mk-II Gas Box divertor. On two occasions during that period a number of limiter and divertor tiles were retrieved from the torus and then examined ex-situ with surface sensitive techniques. Erosion and deposition patterns were determined in order to assess the material erosion, material migration and fuel inventory on plasma facing components. Tracer techniques, e.g. injection ^{13}C labelled methane and tiles coated with a low-Z and high-Z marker layer, were used to enhance the volume of information on the material transport. The results show significant asymmetry in distribution of fuel and plasma impurity species between the inner (net deposition area) and the outer (net erosion) divertor channels. No significant formation of highly hydrogenated carbon films has been found in the gas box structure. The results are discussed in terms of processes decisive for material migration and the influence of operation scenarios on the morphology of the deposition zones. Comparison is also made to results obtained following campaigns with previous divertors.

1. INTRODUCTION

Material lifetime and fuel inventory in Plasma Facing Components (PFC) are decisive for economy in operation of a reactor-class device [1]. It has been recognised that the divertor geometry and the related power deposition profiles have a strong impact on the material transport and its re-deposition. For that reason, an important mission of the JET tokamak is to optimise the wall and divertor geometry and to test a variety of plasma operation scenarios. Over the last decade the main chamber wall and divertor of JET have been restructured several times. Since 1994 it has been consecutively operated with the following divertors: Mk-I with Carbon Fibre Composite (CFC) and then with beryllium tiles, Mk-IIA, Mk-II Gas- Box (GB), Mk-II Septum Replacement Plate (SRP) with CFC tiles in the three Mk-II structures. Following experimental campaigns with those divertors wall components have always been studied in detail [2-8]. Deep insight into the material migration and fuel inventory became absolutely indispensable after the full deuterium-tritium experiments in JET [9] and TFTR [10] when the long-term tritium retention reached about 30% of the cumulative input of tritium [11]. The most pronounced accumulation was found in the inner corner of the Mk-IIA divertor, in particular, in remote areas shadowed from the direct plasma line-of-sight [7,12-15]. Formation of fuel-rich and flaking films on the water-cooled louvres in the pumping duct dominated the overall inventory [7]. From the fact that the layers deposited in remote areas contained vast amounts of hydrogen isotopes and carbon, but no beryllium, one concluded that their presence was associated with chemical erosion of carbon and long-range transport of hydrocarbons [7,15]. Beryllium, physically sputtered from the main chamber wall, was transported to the target plates where it remained. No re-erosion occurs due to the low electron temperature in the inner divertor. The result implied that in the machine with a beryllium wall in the main chamber, fuel inventory related to carbon erosion and C_xH_y redeposition could have been significantly reduced due to the elimination of the major carbon source. It became also important to verify, whether the change of

the divertor geometry – from an open (Mk-IIA) to a more confined (Mk-IIGB) – influences the transport and related deposition pattern. Therefore, the aim of this work is to give a comprehensive overview of deposition profiles and fuel inventories following the operation with the Gas Box divertor. Particular emphasis is given to the study of the inner and outer gas-box tiles, because the box structure could be – to some extent – considered as a remote area for deposition of eroded species and is analogous to the ITER septum.

2. EXPERIMENTAL

2.1. JET AND THE GAS BOX DIVERTOR CAMPAIGN

2.1.1 Tile histories

JET is operated with PFC made of carbon (CFC, Concept I manufactured by Dunlop Ltd). The main chamber wall is coated once per operation week with a thin beryllium layer produced by evaporation using either two or four Be evaporator heads located in the equatorial plane of the torus. Fig.1 shows the vacuum vessel with the Gas-Box divertor, whereas the divertor poloidal cross-section and typical field lines are depicted in Fig.2(a). The inner wall of the divertor comprises Tiles 1 and 3, whilst Tile 4 is at the base of the inner divertor leg (and can be accessed by the plasma only over a limited area. Tiles 7 and 8 form the outer divertor wall, whilst Tile 6 is at the base of the outer leg and, like Tile 4, can only be seen by the plasma in a limited region. The septum is protected by its own tiles, which are numbered 5.

In-vessel components can be retrieved from the torus only during major scheduled interventions connected with the reconstruction of PFC and the installation of new diagnostics. The contamination of the vacuum vessel with beryllium and tritium means the invessel work (including the retrieval of samples) is carried out by Remote Handling using a remotely controlled robotic arm [16].

The Gas Box divertor (Mk-IIGB) was first installed in 1998 during the Remote Tile Exchange (RTE) shutdown, in exchange for the Mk-IIA divertor tiles that were in use 1996-1998 (including the Deuterium-Tritium Experiment (DTE-1) in 1997). During the period with the Mk-IIGB configuration there was an intervention in 1999 when a poloidal set of divertor tiles was removed from Octant 5D and replaced with a special set of marker tiles (see section 2.2). Operations with the Mk-IIGB were completed in Feb 2001, as seen in the time line in Fig. 2(b), and in the subsequent 2001 shutdown a changeover was made to the Mk-II SRP divertor in which the septum was removed and replaced with a cover plate. The special marker tiles installed in 1999 were retrieved for analysis during this shutdown, and thus septum tiles and support structure became available for analysis. At the same time, a new set of marker tiles was installed at Octant 5C and the poloidal set of tiles it replaced was removed for analysis.

Thus three poloidal sets of divertor tiles have been analysed, each characteristic of a different length of exposure time. Firstly, a set was exposed 1998-1999 (Set A), secondly, a set of special marker tiles was exposed during 1999-2001 (Set B), and thirdly, a set was exposed throughout the lifetime of the Mk-IIGB divertor, i.e. during 1998-2001 (Set C).

2.1.2. Mk IIGB campaign details

The most common plasma configurations during the Mk-IIGB operations have the strike points on the vertical Tiles 3 and 7, as shown in Fig. 2, though the location varies, as shown in Fig. 3. The histogram in Fig. 3 also shows that very occasionally the strike point was moved onto Tiles 1 and 8. If the X –point was lowered too much, then one or both of the strike points is intercepted by the septum tiles. It was avoided as far as possible, since the septum tiles did not have as high load-bearing capabilities as the other divertor tiles. However, there was a limited range of plasma configurations that allowed JET to run with the strike points on Tiles 4 and/or 6. Most of the surfaces of Tiles 4 and 6 can be seen from Fig. 2 to be horizontal, but the possible strike point positions were restricted to the sloping parts of the tiles between horizontal parts shadowed by the septum structure and by Tiles 3 or 7. These plasma configurations ("corner shots") were quite frequently run in studies of divertor physics, as they mean that access to the cryopump (which is via the louvres in the corners of the divertor) was from the scrape-off layer (SOL) rather than the private flux region. Corner shots were also believed to be very important for material transport and retention, as will be discussed in section 7.

The vast majority of discharges in JET were fuelled with deuterium, and ran with a fixed direction for the toroidal magnetic field and plasma current. Occasionally there were periods of operation with protium (e.g. for H isotope changeover experiments) or helium fuelling. Unfortunately, such periods were usually at the end of the campaign prior to a shutdown, since protium or helium fuelling produces negligible neutrons, so the vessel activation is minimised. As an example, the four weeks of operation prior to the 2001 opening were in He [17], apart from the last three days which reverted to D fuelling. Since the region best analysed is the near-surface which reflects the latter stages of the plasma operations, such pre-shutdown deviations from normal running make the analysis of PFCs for retention of deuterium much more difficult.

As will be shown later, the normal direction for the toroidal magnetic field and plasma current results in heavy deposition of impurities at the inner divertor, and most areas at the outer divertor exhibiting small amounts of erosion. JET can also operate with the magnetic field and the direction of the plasma current reversed (which is referred to as "reversed field" operations), and there was a short period of JET operation in this mode in 1998-1999 (just before the 1999 shutdown). In reversed field operations, ion temperatures and fluxes at the two divertor legs are more equitable"[35]. It is believed that the deposition of impurities is also more equitable. However, JET has never run a complete campaign in this mode to be sure. It may be that, if there are small differences in deposition patterns between outer divertor tiles of Sets A and B that the reversed field experiment is responsible.

JET has normally operated with a vessel wall temperature of 320^{o}C. The divertor structure is, however, water-cooled in order to protect the poloidal field coils that are situated within the vessel alongside the divertor to produce the necessary field shaping. The divertor tiles are supported by the support structure, but there is limited thermal conduction between tiles and structure. The divertor tiles thus have a base temperature intermediate between the water and vessel temperatures.

Thermocouples are embedded in some of the tiles that continually monitor the (bulk) tile temperature. As can be seen from Fig.4, during the MK- II Gas Box operations in 2000 Tiles 1 and 3 had base temperatures of 170^{o}C and 160^{o}C, respectively. During each plasma discharge (in the divertor configuration) power is deposited on the tile surfaces: the strike point region may reach 1000^{o}C or greater and the overall power deposited in the divertor may be 10 MJ. Thus, during a day of plasma pulsing the bulk temperature of the tiles steadily increases, typically to 210^{o}C and 220^{o}C for Tiles 1 and 3 respectively, as seen in Fig. 4, returning to the base temperature overnight. However, since beginning of 2001 (when the vessel temperature was reduced for safety reasons) the vessel temperature was held at 200^{o}C throughout the two months' operations in 2001 prior to the shutdown. As can be seen in Fig. 4 this means the mean tile temperatures for both Tiles 1 and 3 before and after a day of pulsing are 80^{o}C and 140^{o}C, respectively. It may be that this temperature change has a significant effect on the deposition at the inner divertor, as will be discussed later.

2.1.3. Ion fluxes to the inner divertor tiles

The MkIIGB tiles were facing the plasma for 61470, 101821 and 163291 seconds, including 36870, 57429 and 94299 seconds of X-point discharges for Sets A, B and C respectively. Ion fluxes during pulses are routinely measured with divertor Langmuir probes. Integrated ion fluxes were calculated for the experimental periods 1998-1999 (pulses 44659-48596) and 1999-2001 (pulses 48597-54345), and hence for the combined period 1998-2001 (pulses 44659-54345). The results for the inner divertor wall probes 1-9 are given in Table 1. Probes 1-4 and 5-9 correspond to Tiles 1 and 3, respectively. For tile 1 numbering of the probes is the same as that for the mechanical measurement points in Fig. 2. However, there are 5 probes in tile 3 so the numbering of the probes does not quite correspond to the location of mechanical measurement points. Unfortunately, probe 1 was not working, hence the zero signal level. Ion fluxes seem to be higher for Tile 1 during 1999-2001 campaign than for 1998-1999 campaign. For Tile 3 ion fluxes are quite comparable for both campaigns.

2.1.4. ^{13}C puffing experiment

An active injection of material transport markers was carried out on the last operation session with the Mk-IIGB divertor. ^{13}C labelled methane ($^{13}CH_4$) was puffed into the scrape-off layer from the gas inlet module GIM-5 at the top of the vessel. The key objective for the experiment was to assess the direction of material migration and the resultant location of redeposition. During fifteen ohmic pulses 1.3 x 10^{23} $^{13}CH_4$ molecules were injected, which was judged to be close to the maximum that could be injected without seriously modifying the pulse parameters. The number of ^{13}C atoms puffed into the SOL (assuming no loss of material by deposition local to the nozzles) was therefore also 1.3 x 10^{23}. At the same time silane (SiH_4) was injected from the outer divertor ring (GIM-10) of the torus using 1% SiH_4 mixed with deuterium. However, similar flow rates for the SiH_4/H_2 as for the $^{13}CH_4$ meant two orders of magnitude less Si, and this was found to be too small to give

reliable levels of deposition above the Si background concentration in CFC [18]. The use of minute quantities of injected silane followed the risk assessment related to high reactivity and pyrophoric properties of that gas.

2.2. MARKER TILES

In the 1999 shutdown so-called marker tiles were installed in several locations replacing regular divertor and limiter components. A full poloidal set of six divertor tiles (excluding the septum tiles) was installed, as well as six Inner Wall Guard Limiter (IWGL) tiles and four Outer Poloidal Limiters (OPL) tiles in the main chamber, as shown in Fig.5. The marker tiles were the normal CFC tiles coated with a stripe of sandwich-type thin layers: 2.5μm of carbon-boron (10 at %B) film on top of a 650nm thick rhenium layer. The coatings were prepared by Plansee AG, Austria. The heavy metal interlayer allows the thickness of the carbon-boron layer (and the rhenium layer itself) to be determined with the Ion beam Analysis (IBA) techniques (see next section).

Amounts of deposition and (small amounts of) erosion are determined by comparing the position of the Re and B relative to the surface before and after exposure in JET. The amount of boron remaining in the films after exposure also allowed small amounts of erosion of the carbon-boron layer to be determined. Since rhenium is a high-Z metal characterised by a high energy threshold for sputtering by hydrogen ions, loss of this layer as well as the overlaying carbon-boron would indicate a contribution to the erosion process from either plasma impurity ions or highly energetic neutrals/ions from charge exchange. If there is gross erosion, all trace of the markers may disappear. To cope with this possibility a number of slots were milled in one poloidal edge to act as reference points. Distances to the tile surface from these slots were measured with a micrometer before and after exposure. The accuracy of the mechanical measurements is estimated to be ± 10μm. Figure 6 shows schematically the appearance of a marker tile before its installation in the divertor. The IWGL and OPL marker tiles did not have the milled reference slots. Figure 6 also shows that the divertor tiles were in fact coated with two identical stripes. When these tiles were being prepared, the only divertor tile analysis was from the JET Mk-I divertor [4]. In the Mk-I divertor there were big differences in analysis between the areas of tiles directly exposed to ions travelling along field lines, and the areas of comparable size that were shadowed from impact by the edge of the adjacent tile [4,5]. The same “roof tile” principle for protecting edges is used for tiles in the various Mk-II divertors, thus, a second stripe was deposited on the shadowed edge. However, the Mk-II tiles are much larger in the toroidal direction, so the fraction of shadowed area is much smaller. Mk-IIA tile analyses showed that this shadowed area can be disregarded, hence no data from the shadowed areas of Mk-IIGB divertor tiles will be included in this paper.

2.3. ANALYSIS TECHNIQUES

2.3.1. General

The aim of analysis is to determine the quantitative composition and structure of the surface and near-surface layer of PFCs, i.e. usually CFC tiles in case of JET. The amount and distribution

(spatial and depth) of deuterium, carbon (^{12}C and ^{13}C), beryllium, boron and metals (Re marker and Inconel® components: Ni+Cr+Fe) are of primary interest. No single analysis method can possibly provide the complete data required, and there would in any case be a benefit in comparing analyses from different techniques. Because of problems with beryllium and tritium contamination in samples coming out of JET, we are limited to two sets of techniques with facilities dedicated to that work; Secondary Ion Mass Spectrometry (SIMS) and accelerator-based IBA methods. These techniques are almost unique in their ability to analyse H-isotopes, but access to alternative techniques such as Auger electron spectroscopy and SEM combined with Wavelength Dispersive X-ray Spectroscopy (WDS) would be helpful for other elements, and is planned for the future.

As stated in the previous paragraph, all materials retrieved from the JET vessel are contaminated with beryllium and tritium. Therefore, ex-situ examination of tiles is carried out in controlled areas equipped with glove boxes for transfer and handling of samples. Detailed analysis is carried out in facilities in the Accelerator Laboratory at the University of Sussex in Brighton, UK, and in the Technical Research Centre of Finland (VTT) and in the Accelerator Laboratory at the University of Helsinki, Finland. The facility in Brighton allows, in most cases, for analysis of entire tiles without cutting them into smaller pieces, whereas at VTT smaller samples required for SIMS analysis (cylinders 17mm in diameter) are machined by a coring technique. Figure 7 shows both facilities and sample preparation procedure. The coring technique was also used previously [12-14] when preparing specimens from highly tritiated tiles after the DTE-1 campaign with the MkII-A divertor.

2.3.2. Ion beam analysis techniques

IBA methods used in the study include Nuclear Reaction Analysis (NRA), Rutherford Backscattering Spectroscopy (RBS), Enhanced Proton Scattering (EPS), Particle Induced X-ray Emission (PIXE) and Time-Of-Flight Elastic Recoil Detection Analysis (TOF-ERDA). Data in Table 2 summarise the most typical parameters of the IBA methods. In this work the most demanding was the analysis of ^{13}C in the presence of significant ^{12}C background in the tiles. Therefore, the quantity of ^{13}C re-deposited on the tiles was cross-checked with three independent methods. In case of materials from JET the most convenient is the use of NRA technique based on the ^{3}He(^{13}C,p)^{15}N reaction [19]. Very reliable results are also obtained using enhanced proton scattering ^{13}C(p,p)^{13}C with a 2.5MeV proton beam [20]. The greatest sensitivity is achieved with a proton beam at the resonance energy (1.442MeV) but reliable quantification in this case is possible only for very thin films containing the ^{13}C isotope [21].

Some selected samples that had been analysed by SIMS were also measured with TOF-ERDA to obtain elementary concentrations at the near surface region. In the measurements, the 5MV tandem accelerator EGP-10-II of the University of Helsinki was used with a 53MeV beam of $^{127}I^{10+}$ ions. The detector angle was 40^{o} with respect to the ion beam and the samples were tilted relative to the beam direction by 20^{o}. When a primary ion collides with an atom in the surface, the atom may be ionised and recoil towards the detector with an energy dependent on its mass. The ion will

also lose energy according to the distance it travels through the material before reaching the surface. Thus by measuring the mass and energy of the ions knocked out of the surface, it is possible to derive the concentration with depth into the surface for each isotope. The maximum measured depth is different for every recoiled element and for each matrix because the ion will have a different rate of energy loss with distance travelled through the matrix. However, as an example, TOF-ERDA gives quantitative data for deuterium up to a depth of about 900nm in a carbon-based matrix with 53MeV I^{10+} ions when a density of 2.0g/cm^3 is assumed.

2.3.3 Secondary ion mass spectrometry

SIMS analysis was made with a double focussing magnetic sector instrument (VG Ionex IX- 70S). A 5keV $O2^+$ primary ion beam was used and the ion currents of secondary ions $^1H^+$, D^+, $^9Be^+$, $^{10}B^+$, $^{12}C^+$, $^{13}C^+$, $^{58}Ni^+$ and $^{185}Re^+$ were profiled. ^{13}C and ^{28}Si were profiled separately using a higher mass resolution of 2000 (m/Δm at m/q = 28) to separate the element peaks from the interfering isobars (e.g $^{13}C^+$ from $^{12}CH^+$ and $^{28}Si^+$ from $^{12}CO^+$, $^{12}C_2H_4$). The current of the 5keV O_2^+ primary ions was typically 500nA during depth profiling and the ion beam was raster-scanned over an area of 300° × 430μm^2. Since the surface topography of the CFC tiles varies, SIMS measurements are repeated at several points on each sample, covering an area larger than the fibre plane separation. Profilometer measurements of a redeposited carbon layer and a Be-rich layer allowed the determination of the layer thicknesses and, in a consequence, the assessment of sputter rates in SIMS. Sputter rates used in the calculations are 1.3nm/s for a Be-rich layer, 3.1nm/s for the C-rich layer on divertor Tiles 1 and 3, and 2.1nm/s for the C layer on Tile 4. Relative uncertainty of the sputter rates is estimated to be ± 15%. The roughness of the CFC surface causes the rounded shape and broadening of the SIMS depth profiles, because secondary ion signals come from different depths. This evidently induces variation in the layer thicknesses. It may also change the signal intensities slightly.

3. RESULTS

3.1 MECHANICAL MEASUREMENTS

The results of the micrometer measurements on the poloidal set of divertor tiles are shown in Fig.8. SIMS results for two different divertor tile sets are also included. The numbering of the measurement points (1-24) is shown in Fig.2, as well as the tile numbers (1-8). The thickness of the deposit on the inner divertor wall increases towards the bottom, reaching a maximum of ~90μm. There are even thicker deposits on the small sloping section of the floor that can be accessed by the plasma both at the inner and outer divertor legs (points number 10 and 16, respectively). Note that the bars indicating the micrometer measurements at these two points are in two sections. All other quoted micrometer values are an average of at least three measurements at that point, and repeatability was excellent. However, at points10 and 16 each measurement gave a smaller value than the preceding one, so that after about fifteen measurements the value had reduced by ~50% (indicated by the change in

the bar height). This suggests that the film is dusty in nature, and compresses with successive micrometer measurements. Only small amounts of erosion/deposition are found elsewhere in the outer divertor. The results indicate that the amount deposited in the inner channel exceeds the amount eroded from the outer divertor.

Though the thicknesses of the deposits obtained in SIMS measurements agree reasonably well with the micrometer measurements there are, however, certain differences between results of the two methods. At the inner divertor micrometer results increase towards the bottom. However, although the SIMS results show more deposition on Tile 3 than on Tile 1, the amounts decrease towards the bottom of each tile. SIMS results for the Sets C and B are internally consistent, as the deposits on the former are thicker than those exposed in 1999-2001 (Set B), and were one year longer in the torus. One reason for the difference between micrometer and SIMS results is that the slots used in micrometer measurements are at the edges of the tiles, whilst the SIMS samples were cut from the centre of the tiles. In addition, the SIMS samples do not all come from exactly the same poloidal locations as the slots, and there may be inhomogeneity both in toroidal and poloidal directions. On the floor shadowed by the septum (points number 12-14) there is very good agreement between results of the two methods.

3.2 EROSION – DEPOSITION PATTERN AT THE INNER CHANNEL OF MK-IIGB DIVERTOR

3.2.1. Film structure for tiles exposed 1999-2001

The analysis of the inner divertor wall tiles is the most interesting and the most complex in the vessel, for this is where the major deposition occurs, and where transport processes leading to the deposition into shadowed region must begin. The general film structure for Tiles 1 and 3 of Set B as analysed by SIMS is shown in Figs.9 and 10, respectively. The raw data from which Figures and 10 are derived from the count rate (Y-axis) plotted against sputtering time (X-axis). The sputtering time has been converted to microns in the figures based on measurement of crater depths for a number of SIMS analysis points, assuming that the sputtering rate remains constant through the various layers: there may be errors of up to 50% in this calibration. In summary, the surface film for Tiles 1 and 3 from that set comprises a number of layers. Firstly, at the very surface is a thin layer containing ^{13}C deposited during the last pulses of the campaign when $^{13}CH_4$ was puffed into the vessel. Secondly, the outer region of the major part of the film is predominantly carbon (^{12}C) with a high deuterium content and some beryllium (and other metallic impurities). Thirdly, the inner region of the deposited film is very rich in beryllium (and other metallic plasma impurities such as nickel), with a relatively low D content. Finally, on the regions of the tiles pre-coated with the stripe of C+B and Re interlayer, the elements B and Re appear as peaks at the interface with the carbon (CFC) substrate.

The samples analysed by SIMS illustrated in Figs 9 and 10 were cut from near the bottom of Tile 1 and near the centre of Tile 3 (poloidal positions 4 and 7 in Fig.2), respectively. The analysis points

were on the pre-coated stripes, so the Re and B-containing marker layers are present at the interface between the deposited film and the CFC substrate; the Re signal is included in Fig.9. The outer layer (approx. 2-6μm thick on Tile 1 and 10-16μm on Tile 3) contains mostly C and Be together with deuterium. The composition deeper into the deposit of the Tiles 1 and 3 is quite different to the surface composition. It shows that the majority of the film (from 4 –12μm at point 4 and 13 –32μm at point 7) is very rich in beryllium, and nickel also peaks in this region, as shown in Fig.10. Layers rich in metals, and depleted in carbon, have been found at the inner divertor wall previously [7]. It must be pointed out that there is high amount of oxygen in the Be-rich layer according to RBS analyses which increases the secondary ion yield and signal intensity for Be.

The amounts of ^{13}C found on the various samples at the inner divertor are plotted in Fig.11. They are derived by calibrating the surface ^{13}C peak in SIMS with the amounts of ^{13}C found by TOF-ERDA on a sub-set of the same samples. Whilst the overall film thickness measured by micrometer increases markedly in the lower half of Tile 3, as shown in Fig. 8, the amount of ^{13}C measured on Tiles 1 and 3 (Fig.11) is much reduced at the bottom of Tile 3. This may be because the ^{13}C is mostly ionised deep in the SOL (measurements from another work suggest the maximum occurs at 20mm from the LCFS), with relatively little reaching the separatrix [22], and then travels along the SOL to the inner divertor. The strike point for the discharges in the puffing experiment was about one-third the way up Tile 3, so this should be the cut-off point for the ^{13}C distribution, if no migration occurs at the tiles. Integrating the amounts of ^{13}C measured on Tiles 1 and 3, and assuming these particular tiles are typical of the full toroidal set, gives 4.8 x10^{20} atoms compared to the 1.3 x10^{21} atoms injected, or about 37% of the ^{13}C input.

For IBA, the film on Tile 3 is so thick that since IBA generally sees the outer few microns, it can only analyse the outer part of the film. RBS spectra from tile 3 are difficult to interpret, as the background is affected by the large change in composition deeper into the surface, however the thinner layers on Tile 1 give RBS spectra in which the layers are resolved. The two films (and also the surface deposition of ^{13}C) have been simulated with the SIMNRA program [23] for many RBS spectra from Tile 1. Fig.12 shows the experimental and the simulated RBS spectrum for a point towards the bottom of the tile.

First attempts here to model the deposited film use three different layers in the simulations, since there are clearly at least three identifiable layers from SIMS data; a thin outer layer containing the ^{13}C, and the two parts of the main film. The thickness and ^{13}C content of the outer layer is determined by the fit to the ^{13}C feature indicated in Fig. 12, whilst the second layer thickness and ^{12}C content is first estimated by getting a reasonable fit to the ^{12}C feature arrowed in the spectrum. The thickness of the third layer is first estimated by fitting the width of the Be feature in the figure, then the Be and C contents of the various layers are adjusted iteratively until a best fit to the overall spectrum is obtained. The results of the simulation at this stage, which gives the fit shown in Fig.12, are collected in Table 3. The error of stopping powers and cross section data is typically about 5%, resulting in a systematic error of 5-10%, which is much larger than the inaccuracy of the fit. It

would no doubt be possible to improve the fit a little by increasing the number of layers, but the process is extremely laborious, and the fit in Fig.12 is considered to be adequate.

RBS data are based on atomic scattering cross-sections, so are calibrated against numbers of atoms in the films. To convert to thicknesses in microns it is necessary to use the various film densities, which are not well known for deposited films in tokamaks. The conversion factor commonly used is 1 micron equivalent to 10^{19} atoms cm^{-2}, which is simple to remember, and close to the theoretical densities for C and Be. However, the densities of films deposited in tokamaks are probably significantly lower. For example flakes of deposits from the JET divertor have a measured density of 1.6g cm^{-3} [24]. This would give 10^{19} atoms cm^{-2} is equivalent to 1.25microns. Using this value, the thicknesses of the three films listed in Table 3 are 0.34 2.6 and 2.6microns, respectively. It must be admitted that there is some inconsistency with the thicknesses derived from SIMS profiles. However, qualitatively the RBS spectrum is totally consistent with the SIMS three-layer picture of a thin ^{13}C layer on top of one layer rich in ^{12}C and D and a second layer on the surface of the CFC substrate containing carbon and a large fraction of beryllium oxide.

3.2.2. Comparison of tiles from the various Mk-IIGB phases

As mentioned previously, tiles exposed in JET 1999-2001 and 1998-2001 (i.e. Sets B and C) have been analysed both by SIMS and IBA, whilst additionally tiles exposed 1998-1999 (Set A) has been analysed only by IBA. Deposition on tiles of Set C could logically be assumed to comprise the film seen after the 1999-2001 exposure on top of that seen after the 1998-1999 exposure. Furthermore, if the impurity fluxes are proportional to the ion fluxes shown in Table 1 (section 2.1.3), then one expects only a small contribution from the 1998-1999 campaign to the combined deposition for Tile 1, but roughly equal contributions from 1998- 1999 and 1999-2001 operations for Tile 3.

The previous section showed SIMS results for Set B of divertor tiles. The SIMS profiles for Set C looked very similar, but for both Tiles 1 and 3 both the inner and outer films were on average a factor 1.6 thicker. Since both sets of tiles were exposed to the same ^{13}C puffing experiment, the amounts of ^{13}C would be expected to be the same. However, according to the SIMS analyses the amounts of ^{13}C over Tiles 1 and 3 was also a factor of ~1.7 greater for Set C than the tiles of Set B. If this value is used to estimate the total amount of ^{13}C found in the divertor, then of course the amount is greater than in the previous section, and would account for about 63% of the ^{13}C puffed into the vessel. This may be related to toroidal asymmetries in deposition and will be discussed later.

A similar comparison for Tile 1 has been made by RBS. Figure 13 compares spectra from similar points, towards the bottom of the front face of Tile 1, for Set A (JET 5610), B (JET 7103) and Set C (JET 6877). The ^{13}C peak, and the onset channel for the ^{12}C feature (marking the surface) are the same for spectra JET 6877 and JET 7103. However, the height and width of the ^{12}C feature in JET 6877 spectrum is clearly greater than in JET 7103, indicating a bigger outer C+D film, and the onset of the Be feature is thus at lower channel number (further from the surface). In JET 5610

there is only a very narrow Be feature, implying a thin Be-rich layer, and the onset energy of the feature is the maximum possible for Be (the “Be edge”), showing that the Be was present from the very surface of the tile. For the other spectra in Fig.13 (also used in Fig.12) the Be feature is shifted to the left, i.e. towards lower energy, meaning that the Be is covered by another layer which absorbs beam energy before it reaches the Be. Thus the C-rich layer seen in JET 7103 on top of the Be-rich layer is missing in JET 5610, and is characteristic only of tiles that were in JET in 2001. The ^{13}C layer which is too thin to affect the positions of other peaks is also missing, since the ^{13}C was only added to JET on the last day of operations in 2001. The Be feature in JET 6877 is also larger than that in JET 7103, as inferred from the width of the Be feature. Therefore, the inner C- and Be-oxide film is also greater for the tile exposed for the longer period. The D features in the outer film for spectra JET 6877 and JET 7103 are similar.

Spectra for a number of similar pairs of tiles have been simulated with the SIMNRA fitting programme, and the results consistently show that both the C- and D-rich outer layer and the C- and Be oxide-rich inner layers are a little thicker for samples from tiles exposed 1998-2001 than for tiles exposed from 1999-2001. Integrating all the Be in the films, typically there is about 50% more in the sample exposed for the longer period.

The overall thickness of the double layer at these points on Tile 1 are 5.4 10^{19} atoms cm^{-2} for Set C and 4.13 10^{19} atoms cm^{-2} for Set B. Using the same approximation as used above that 10^{19} atoms cm^{-2} corresponds to 1.25μm, the film on Set C is about 1.6μm thicker.

In an effort to calibrate the Be signals for IBA (and also for SIMS) foils have been obtained from Goodfellow Metals Co. of 0.25, 1.0 and 5μm Be on copper backings. It is to be assumed that these foils are fully dense, with an atomic density of $10^{19}cm^{-2}$ per micron film thickness. The Be feature in the RBS spectrum from the 1μm film had a half-width of 17 channels, compared with 18 channels for the feature in JET 5610. The 0.25μm films gave a peak of half-width 9 channels, but only 60% of the peak height, showing that much of the 9 channels half-width is broadening due to the energy resolution. Thus the Be peak shape suggests the Be-rich film in JET 5610 is somewhat variable in thickness, but with a mean just over 1.25μm (allowing for the lower film density): this may be compared with the difference in thickness of the spectra in Fig.13 of ~1.6 microns. These results are summarised in Table 4.

The IBA variant NRA has also been used to investigate the films on the inner divertor tiles. Fig. 14 shows dramatically the difference between the surface of the centre of Tile 3 in Set A (JET 5573) and the centre of Tile 3 in Set B (JET 7021). The spectrum from the tile removed in 2001 (JET 7021) shows a large D feature and a relatively small Be peak, whereas in 1999 (JET 5573) the surface contained much more Be and much less D (relative to the C peak). The Be/C ratio derived from JET 5573 is 1.21, and this value is in line with analyses of Mk-IIA divertor tiles [7]. (Unfortunately the samples removed in 1999 were returned to the vessel in the 2001 shutdown, so cannot be analysed by SIMS.). By contrast the Be/C ratio derived from JET 7021 (removed 2001) is only 0.12. Since the outer part of the duplex film on Tile 3 is much thicker than the NRA analysis

depth (which is typically 1-3 microns for C and Be), this analysis is of the outer film. The average Be/C ratio for 27 measurements on Tile 3 samples removed in 2001 was 0.137.

NRA of any tile 1 removed in 2001 shows greater Be/C ratios due to the influence of the inner Be-rich film, but has no depth resolution to allow separation of the layers (unlike RBS).

3.3 EROSION – DEPOSITION PATTERN AT THE FLOOR OF MK-IIGB DIVERTOR

Mk-IIA tiles showed thick films of high D/C ratio with no Be and other metallic impurities on the part of Tile 4 shadowed by Tile 3 [6,7,15]. Similar films are seen in Mk-IIGB, and are about 50μm thick, as was seen in Fig. 8. Somewhat thinner films (~ 15μm) are also seen in the region of the Mk-IIGB Tile 4 shadowed by the septum. In this region the films have a D/C concentration ratio of ~0.4 and also negligible Be and other metallic impurities.

In the more central region of Tile 4, including the sloping section of the tile (see Fig.2), D contents are much lower and sometimes concentrated at the surface, and traces of Be are visible. From the IBA spectra of the surface region, there is no indication that there is a very thick friable deposit (~200μm) seen with the micrometer and SIMS over just a part of the area (point 10 in Fig. 2). However, this thick deposit, which is present at the extreme corner of the divertor accessible by the plasma, may be the key in understanding material transport, as will be discussed in section 4. A similarly friable film was present at the equivalent point in the Mk-IIA divertor, and shows up clearly in infra-red [25] and tritium mapping [26] experiments, but its thickness was not determined.

Sets B and C have been analysed by IBA and SIMS. Since the present understanding is that carbonaceous material arrives at these regions and is then not disturbed by the plasma, if a tile has been exposed for twice as long, then the films should be twice as thick. However, in the area shadowed by Tile 3 (point 9 in Fig. 2) SIMS estimates that the film deposited during 1999-2001 is significantly greater than that deposited over the longer period. Furthermore, on the part of tile shadowed by the septum the carbon-based film deposited during 1999-2001 on tiles of Set B appears by NRA analysis to be > 7 microns thick in places, whilst for the tile of Set C the film everywhere is <7 microns thick. These differences are most likely due to toroidal variations, as also discussed in section 4.

The outer base Mk-IIGB Tile 6 shown in Fig.15 also has a narrow thick, friable band on the sloping region (point 16). This is the extreme point of access for the plasma into the corner of the outer divertor, analogous to point 10 for the inner divertor. A sharp change of film structure is visible by eye towards one edge of this sample. From the NRA spectra it is clear that there is a thick film with rather high D/C ratio on the sloping part of Tile 6, but this rapidly attenuates to a surface (~2μm) film near point 17. Towards the septum (from point 15 to 14), all samples show just a surface film of modest D concentration. In Fig. 16 there is a typical RBS spectrum from this region (near point 14). Comparing with spectra from coated tiles before exposure (JET 5293), it is apparent that the Re is again located ~2μm below the surface, but is somewhat reduced in amount, and that there is D in the surface layer. This agrees well with the SIMS depth profiles (see Fig.17) which

also shows D in a surface film 2μm thick below which is the Re layer, together with B and some Ni. However, although it shows that the Re is in the same location relative to the surface, we are not merely seeing the original coating. There is a sharp change in composition (e.g. of the Re) at a depth of about 2μm. Beyond that there is intermixing of the Re and B from the C/B coatings (and some Ni from within the tokamak), and we know from the RBS there has been erosion of some of the film. On top there is a layer of carbon and deuterium, which has perhaps been deposited more recently at lower temperature, since there is no mixing of Re into this layer. Thus what at first glance from the RBS spectra seems comparatively simple is in fact rather complex.

3.4 EROSION – DEPOSITION PATTERN AT THE OUTER WALL OF MK-IIGB DIVERTOR

Analysis of the coated stripes on the marker tiles installed at the outer divertor wall (Tiles 7 and 8) and exposed 1999-2001 show erosion at all positions. This is not clear from the micrometer measurements, which show either small dimensional increases or decreases, with an average of approximately no change. However, SIMS analyses show no evidence of the C+B coating, at some points a small amount of Re remains at the surface, and at others none remains. The SIMS depth profile in Fig. 18 recorded from the centre of Tile 7 is typical. It shows some deuterium at the surface, probably from implantation/surface diffusion, but negligible remaining Re, and no detectable deposited ^{13}C. This spectrum is in total contrast to spectra from the inner divertor wall such as Fig. 9 and 10.

Clearly at the outer divertor there is no film being formed from impurities that may be arriving from the main chamber (unlike at the inner divertor), and removal of at least some of the marker film demonstrates there is some net erosion of the original tile surface. The extent of the *erosion* at the outer divertor wall must be much less than the *deposition* at the inner, however, or else there would be clear evidence of erosion from the micrometer measurements. Some of the erosion must be by impurity ions, or by high energy ions of the fuelling gas, in order to sputter Re atoms. Either none of the ^{13}C puffed into the vessel during the last pulses reached the inner divertor wall, or it was unable to settle there. The IBA data are consistent with the SIMS results.

3.5. ANALYSIS OF THE SEPTUM AND GAS BOX TILES

3.5.1. Analysis of septum tiles after exposure in JET 1998-2001

Figure 19 shows the schematic view of the septum and the gas box module. For most discharges the septum tiles are within the private flux region, and have little interaction with the plasma. Occasionally the X-point is placed too close to the tiles, and the inner and/or outer divertor separatrix strikes the tiles. Two tiles (number 5) are mounted on each section of the gas box, and the tiles are shaped to protect the joints between the gas box sections. The highest point of each tile is at a ridge near the joint between the two tiles on the section of gas box, leaving an area of reverse slope to protect the joint between the pair of tiles. Depending on the plasma field direction, the area of interaction of

plasma ions with the tiles is to one side of the ridge on each tile. This results in local re-deposition of material sputtered from the surfaces impinged by the plasma on the lee side of the ridge for each tile. In these areas, which are darker-appearing bands ~25mm wide across each of the ~160mm long tiles, there is a significant concentration of D in the surface region and some low levels of Be contamination, whilst levels are markedly lower elsewhere. There is much more D and Be on the outboard part of the band. On other areas of the tiles, the D and Be levels remain low over the whole width of the tile. In all cases, however, the D and Be are restricted to the near surface (~1μm) layer, so overall the tiles contain very little trapped fuel.

3.5.2 Analysis of Gas Box tiles

The gas box module, as shown in Fig.19, comprises a base plate, a top plate, a set of three vertical support plates in the poloidal plane and two divider plates (in the toroidal plane) creating a separation between the inner and outer divertor channels. There are also a number of other items that cover fixing bolts, join units to adjacent units, etc. All the aforementioned components are made from CFC. There are direct lines of sight into the support structure from the divertor target regions, and it is possible that material sputtered from the targets may travel to the structure, where it would remain since the region is completely shadowed from the confined plasma. The ITER divertor geometry is similar, and a number of diagnostics plan to gain access through the septum structure, so the amount of deposition in this region is highly ITER-relevant.

Surface morphology of all the vertical support and dividers plates of Module 12 was studied with IBA. A dusty deposit was observed near the plate edge facing towards the inner divertor channel. Moreover, there were areas partly eroded by arcing. Analysis was done across the tile and the results for one side of the middle plate are shown in Fig.20. These results confirm that some deposition occurred in narrow belts (15-20mm wide) near the plate edges on the inner divertor side where the deposit is predominantly a deuterated carbon film with the fuel content reaching up to 2.3×10^{19} D atoms cm^{-2}. The amount of trapped fuel on the outer divertor side is distinctly lower, generally not exceeding 2×10^{18} D atoms cm^{-2}. The deposit thickness was everywhere in the range that can be probed by IBA, i.e. not exceeding 8-10 microns. The deposit contains certain amounts of beryllium: $0.1\text{-}2 \times 10^{18}$ Be atoms cm^{-2}.

With one exception, very similar results have been obtained for the end plates of the module. A local area with greater deposition (> 10μm) was found near the base on one side of one end plate. From the analysis of the one gas box module available for this investigation, it is difficult to conclude whether that thicker deposition was toroidally systematic or unique this area. Nonetheless, it does not significantly influence the overall deposition pattern inside the gas box.

Low levels of deuterium and beryllium (less than 1.5×10^{18} atoms cm^{-2}) are found on both sides of the divider plates. Therefore, the results for the support and divider plates are consistent. Moreover, no ^{13}C – above the background level – has been detected on any part of the gas box plates, showing that the material transport to that region is limited. The results give also clear

indication that the gas box components can not be considered as a major place for fuel retention. Additionally, the thin deposit on the dividers proves that the direct material transport across the divertor is negligible, if any.

3.6 EROSION – DEPOSITION SOURCES IN THE MAIN CHAMBER

3.6.1. General

From earlier sections it is evident there is more deposition in the inner divertor than erosion in the outer divertor, and that the source of much of the deposition must be the main chamber. This has been proposed previously [27]. The inner and outer walls of the main chamber of JET are protected from ions travelling along field lines by limiters: IWGL and OPL, respectively, as shown in Fig.5. However, Charge eXchange Neutrals (CXN) may travel from the plasma in any direction, and may thus be able to cause sputtering at any part of the vessel with a line-of-sight to the plasma. In particular it has been shown that significant sputtering occurs at the areas of the inner wall between the IWGL [28] (which for this reason has been covered with CFC tiles). However, it is not clear if enough material can be sputtered from these areas, or whether it would reach the SOL to be transported to the inner divertor, to account for the deposition.

There is evidence that there is interaction between the limiters and the plasma – erosion/deposition patterns at the IWGL are clearly visible in Fig.1 – but no quantitative measurements have been made earlier. As described in section 2.2, in 1999 a number of IWGL and OPL tiles were coated with a Re interlayer and C+B overlayer. The erosion/deposition measurements resulting from the 1999-2001 operations are summarised below.

3.6.2. IWGL analysis

The cross-section of the IWGL limiter is shown in Fig.21. Each limiter is a poloidal array of 19 pairs of tiles, at each position the tiles to the left and right of the centre being labelled “L” and”“R”. The tangency points are to either side of the centre, to protect the tile joint. The three pairs of tiles that were coated, analysed, exposed in JET for 1999-2001 and then re-analysed were indicated in Fig.5. The designation 2X or 3X denotes in which of the sixteen IWGL the tiles were mounted, whilst the numbers 2, 11 or 17 are the poloidal positions (numbering from the top).

IBA and SIMS analyses have been carried out on all six IWGL tiles, and it is clear that there are areas of net deposition, and areas of erosion. Figure 21 shows the amount of erosion/deposition seen from SIMS analyses. Deposition is mostly found on the right-hand side tile near the top of the limiter, being greater than 50μm for each area analysed on tile 2X2R. Near the bottom the left-hand side tile (e.g. 3X17L) is a deposition area, whilst near the centre erosion/deposition is more balanced between the tile pair as shown in Fig.21. Figures 22-24 show the RBS spectrum (JET 6270), NRA spectrum (JET 6293) and SIMS depth profile, respectively from a region of deposition near the centre of Tile 2X2R. This shows that the surface is covered by a deuterated layer of carbon plus some beryllium. The Re-containing layer is clearly visible in the SIMS depth profiles of Fig.24, at

the interface between a deposited film (which is approximately 60microns thick) and the CFC substrate. A total of 30NRA spectra (including JET 6293) have been recorded from areas that SIMS shows have >10μm of deposition. The average B/C ratio derived from these NRA spectra from regions of deposition on the IWGL is 8.3%.

As seen from fig.21, much of the IWGL is covered by quite thick deposit, and in these regions the coated stripe can no longer be seen by eye. Areas of erosion are also widespread, but generally the coated stripe can still be just seen, and part of the Re interlayer is still present. As an example, fig.25 is an RBS spectrum from the tangency point of Tile 3X17R; there is clearly a Re peak which is right at the surface, because there is a sharp leading edge to the feature instead of a shifted (somewhat gaussian) peak. However, the Re feature is smaller than for the "as-deposited" film shown previously (fig.16, JET 5293). The C edge in fig.25 is not sharp, due to the presence of the Re in the surface layers. The only area that the stripe is not visible due to erosion is at the right-hand side of Tile 3X11L, and from SIMS analysis we see that in this area the coating has been eroded completely.

There are approximately equal areas of erosion and deposition on the six IWGL marker tiles examined. **G**enerally, erosion is limited to removal of the C+B layer and part of the Re interlayer (a total of 2-3microns). This may, however, give an unfair comparison of the erosion and deposition. Most of the interaction with the limiters will be by ions. The vast majority of these will be deuterium ions, which have a high sputtering coefficient for carbon, but at normal incident energies have a negligible probability of sputtering Re. Limited sputtering of Re may occur by impurity ions impacting the surface. It may be that there would be a more equitable picture of erosion and deposition at the IWGL if erosion of uncoated CFC surfaces could be determined, but it remains to be seen whether the IWGL would become a net contributor to deposition in the inner divertor.

SIMS and IBA spectra show traces of ^{13}C at areas of deposition at the IWGL. The amounts are more than an order of magnitude less that at samples from the inner part of the divertor. Furthermore, the area of deposition at the inner wall is marginally less (~4.3m^2 compared to ~5.4m^2) than in the divertor. Therefore, the integrated amount deposited on IWGL may be estimated as about 1 - 2% of the input to the vessel.

3.6.2 Erosion/deposition pattern at the outer poloidal limiters

The positions of the OPL marker tiles mounted in JET in 1999 and exposed during 1999-2001 are shown in fig.5, and a cross-section of a tile is shown in fig.26. As each tile is only 26mm wide in the poloidal direction, the entire plasma-facing surface was coated with the Re and C+B. Ninety-two individual tiles comprise the ~2m poloidal length of the limiter. In practice, each tile is mounted as one of a pair, so each limiter comprises 46 pairs. The pairs are designated such as 2B 01, meaning Octant 2 sector B, position number 01 (which is the top position), followed by whether it is the top or bottom pair at that position. Thus the lowest pair in the limiter is number 23 (bottom). For simplicity the "top" and""bottom" will be omitted from the descriptors.

The general picture for the OPL is erosion from the central region of the tile and some deposition near the ends of the tile as it curves away from the LCFS deeper into the SOL. For the central regions of Tiles 2B01, 2B17 and 8D21 there is some erosion, as indicated by reduced Re and B signals compared to the "as-deposited" films. For Re the reduction is about a factor of two, as shown for Tile 8D21 in Fig.27; the remaining Re is seen by RBS to be at the surface. This is analogous to the situation described for IWGL tiles in the previous section, and illustrated with the RBS spectrum in Fig.25. The Re film has disappeared completely from the central region of Tile 8D09 as seen in Fig.28, also analogous to one area on the IWGL. Tiles 2B01 and 2B17 have similarly reduced amounts in the central region to Tile 8D21. The boron analyses also show that the coating has disappeared completely from the central part of 8D09 (see Fig. 29). Since the Re has disappeared, no estimate of the amount actually eroded from this region can be made. Some boron remains on 2B17 despite the reduction in Re: this suggests there may be some inter-diffusion of B and Re.

Some deposition is found at the ends of the OPL tiles. For Tiles 2B01, 2B17 and 8D21 the amounts are quite small, typically 1-3 microns. For Tile 8D09 small Re peaks are seen by RBS ~50mm from each end (as seen in Fig.28), which then disappear again towards the very ends. The peaks represent a sharp transition from the central area of erosion to an area of deposition. SIMS shows there is a much thicker deposit towards the very end of this tile (see Fig.30, which clearly shows the buried Re-marker layers) than on the other tiles. Thus the reason for the decrease of the Re signal at the very ends of 8D09 in Fig.28 is that the Re marker layer is too deeply buried to be visible by RBS.

Thus the central regions of the OPL tiles are areas of net erosion. Since the marker layer had completely disappeared in this region for the tile near the outer mid-plane, the erosion cannot be quantified. Also, for the upper and lower parts of the OPL, it is not clear how much erosion would occur from other uncoated CFC tiles by deuterium ions, when not protected by a Re layer. Unlike the IWGL, however, significant deposition is limited to a small proportion of the tile near the mid-plane that exhibited the erosion. This is perhaps prompt re-deposition of some material eroded along adjacent field-lines. No surface deposition of ^{13}C was seen at the OPL, even at the region of deposition on 8D09.

4. DISCUSSION

4.1. DUPLEX NATURE OF THE FILMS ON INNER DIVERTOR WALL TILES REMOVED IN 2001

The obvious difference between the analyses of tiles from the Mk-IIGB divertor in 2001 and those analysed previously is the duplex structure of the films on the inner divertor wall. There is an inner layer very rich in Be and other metals, whereas the outer layer is rich in D, but otherwise comparable in composition to films on the IWGL. The surface then has a thin layer rich in ^{13}C from the puffing experiment on the last day of 2001 operations. Note that no duplex structure was seen on Mk-IIGB

tiles exposed 1998-1999 nor on tiles exposed in the Mk-IIA divertor; these tiles only had films very rich in Be and other metals. Thus it appears that there is something different about the exposure of the tiles that were removed in 2001, rather than a difference in the divertor geometry.

As discussed in section 2.1.2 the latter part of the campaign ending in 2001 was different to previous campaigns in two ways. Firstly, throughout 2001 the vessel wall was reduced in temperature from 320°C to 200°C (during which period there were 800 pulses). Secondly, although the final 60 pulses were in D, the previous 400 were in He during a sustained four weeks helium campaign [17]. It was suggested previously that the reduction in wall temperature may be responsible, due to reduced chemical erosion at the inner divertor [8]. Since 2001 JET has continued to operate at 200°C, so the analysis of tiles to be removed in the 2004 shutdown should provide much more definite data.

4.2. COMPARISON OF TILES EXPOSED 1998-2001 WITH TILES EXPOSED 1999-2001

If a new tile is placed into a deposition zone in a region strongly interacting with the plasma, does it retain its individual nature, or become integrated into the surroundings? The inner divertor wall tiles mounted in 1999 (Set B) into a matrix of tiles already exposed since 1998 (Set C) described in this paper (section 3.2.2) are good examples. If the tile is exposed for a longer period, then the overall film thickness might be expected to be greater, but the deposition during the common exposure period should be the same. The evidence from section 3.2.2, does not entirely agree, however:

(i) Langmuir probe data show that integrated ion fluences to inner vertical Tiles 1 and 3 for Set B were 86% and 52% of the total 1998-2001 fluences (i.e. to Set C), respectively

(ii) The thickness of both inner and outer layers on both Tiles 1 and 3 of Set B are roughly 60-65% of that for tiles of Set C

(iii) The amounts of ^{13}C seen on the two sets of tiles are in a similar ratio.

(iv) Deposition on horizontal Tile 4 of Set B is thicker than on Set C

(v) For Tile 1, RBS data suggest the thickness of the film seen on Tile 1 in Set A was approximately the difference in thickness between Tile 1 exposed (at the same location) during 1999-2001 and the film exposed for the combined period in a slightly different location. However, the film in Set A was entirely Be-rich in composition.

The discrepancy between points (i) and (ii) may be resolved by recollecting that Langmuir probe data are dominated by the contribution from deuterium ions. Impurity fluxes do not necessarily have the same distribution, as shown by methane puffing experiments: Langmuir probe measurements made with the reciprocating probe at the top of the vessel suggest the peak C concentration for impurities emanating from the wall is ~20mm (mid-plane equivalent) from the separatrix [22]. This is quite different to impurities exiting the core of the plasma, which would be expected to fall off exponentially with distance from the separatrix as does the D ion flux.

Point (iii) suggests there may be some toroidal variation in the deposition of ^{13}C. Now, a toroidal variation in ^{13}C flux into the divertor may be possible, since the $^{13}CH_4$ was injected from a single

nozzle at the top of the vessel. However, the two tile sets were quite close to each other in the vessel, so it may be the variation is in toroidal tile-to-tile asymmetries rather than flux asymmetries into the divertor. Only toroidal variations seem likely to explain point (iv), however.

Taking point (v) in isolation would suggest the tiles new in 1999 (set B) retain their individual nature, and the films on tiles in set C are a composite of the film on the Set B tiles on top of the film on the tiles of Set A. But tile set C would then have a thicker Be-rich layer and a similar outer layer to set B, and this is not the case (point (ii)). Another possible scenario is that there is a certain amount of erosion and re-deposition of elements at the inner divertor walls (even of Be and other metals) before they are finally buried within the surface films.

Each erosion/re-deposition step involves toroidal transport of the order of centimetres, so the clean tiles installed in 1999 may end up with a typical tile analysis for that poloidal location, not an analysis characteristic only of its period in the vessel. There is support for this view from spectroscopy of probes or tiles of dissimilar material inserted into all-carbon machines such as TEXTOR [30] and ASDEX-Upgrade [31], when almost immediately the spectroscopy from the probe is dominated by carbon, as from nearby surfaces in the machine. Strong spectroscopic signals are seen from Be eroded in the JET inner divertor, so some local erosion and re-deposition must occur - indeed there are similar signal levels from recycling Be seen in the inner divertor to that in the outer. However, it is not clear how this squares with the analysis results that negligible quantities of Be are found in the outer divertor, and large amounts of Be in the inner divertor which do not apparently migrate towards shadowed areas [32].

The factor 1.6 difference in thickness of the films on sets B and C (section 3.2.2) may thus be due as much to statistical variation between sets at differing toroidal location as to difference influence expected from time in the vessel. This makes it difficult to calculate with confidence the amount of transport occurring in the Mk-IIGB divertor in comparison to that in Mk-IIA. The amount of carbon deposited at the inner divertor in Mk-IIA from 1996-1998 was estimated as ~1kg, from the amount of tritium co-deposited with the carbon. Since there was no tritium used in 1998-2001 period, the amount of deposition is being estimated from the Be found on Tiles 1 and 3 (the only sinks for Be). This result is combined with the assumption that on average the Be arriving at the divertor is the same fraction of the average impurity flux as that in the plasma. The dominant plasma impurity is carbon. For the first pulse immediately after a Be evaporation there is a large Be plasma impurity fraction, but this rapidly drops to just a few per cent of the C, and the average Be level is ~8% of the C [32]. Attempts have also been made to correlate Be amounts from tile analysis with calculations of Be flux from spectroscopic measurements for Mk-IIGB [32,36]. The amounts of beryllium and carbon predicted from tile analyses and from spectroscopic data are similar. Both data sets indicate that the average deposition rate during the MkIIGB phase (1999-2001) is perhaps a factor of two lower than during the MkIIA phase (1996-1998), but this factor is similar to the confidence level for the quantification.

4.3 TRANSPORT IN JET DURING CAMPAIGNS WITH THE MK IIGB DIVERTOR

The model for C transport in the Mk-IIGB divertor for the period 1998-2001 (inclusive) remains transport of impurities along the SOL to the inner divertor, followed by chemical sputtering of carbon from the inner divertor wall. A clearer picture of the consequent transport is, however, appearing, if data from deposition monitors [33], the quartz microbalance [34] and the IR camera [35] are combined with the data given here on deposition at the inner corner of the divertor (point 10 in Fig.2). The carbon will proceed in erosion/ionisation/redeposition steps until it reaches point 10. On occasions there is significant plasma power applied to point 10. It may be the strike point is placed in the corner, or crosses the area during a plasma sweep, or there may be a power surge from a large ELM at that point. On such occasions the IR camera records temperatures too high to measure, but indicating ablation of the surface of the dusty deposit, and the QMB has captured one or two such events which seem to give very large amounts of deposition. Thus the final step in transport into the shadowed areas around the louvres is perhaps by occasional intense bursts of carbon particles when power is applied to the large repository on Tile 4. Transport to the septum support is limited to particles sputtered from the inner divertor wall crossing the separatrix into the private flux region without being ionised. Thus the deposition monitor on the septum support will mainly see particles travelling from Tile 3, and the one in front of the inner louvres will collect particles travelling from the sloping part of Tile 4, as observed in each case.

Clearly in the latter part of the 1999-2001 campaign transport within the inner divertor changed. Deposition from the main chamber is still occurring, but the enrichment of Be by subsequent movement of carbon is reduced. NRA analyses show that the average Be/C ratio in the surface film is 13.7% compared with typically equal amounts of Be and C from earlier campaigns [7]. Note, however that the mean Be/C ratio for deposits at the IWGL is 8.3% (section 3.6.1) (which is similar to the mean ratio of Be to C seen spectroscopically in the main chamber [32]). This suggests that some carbon is still being transported from the inner divertor wall towards the louvre region. Let us assume a Be/C ratio of 0.08 for the impurities arriving at the divertor in the SOL. Then, for earlier phases for which the remaining deposits on tiles 1 and 3 give Be/C of ~1.0, it implies 92% of the C is re-eroded. Just prior to the 2001 shutdown, re-erosion of ~42% of the C would produce the Be/C ratio measured by NRA. Thus, despite the dramatic difference in composition of the two layers, the implied flux of carbon to the inner louvre region is only just over a factor two less in the latter stages of the campaign (92%/42%). A factor of about two could feasibly be due to difference in chemical sputtering rates resulting from the divertor temperature change of ~70K from 1998-2000 to 2001 (see Fig 4), given the steep changes in radical formation rates with temperature observed in the laboratory [37].

4.4 FURTHER EXPERIMENTAL WORK IN SUPPORT OF EROSION/DEPOSITION MODELLING

IR data [35] and QMB data [34] suggest erosion or ablation from the extreme corner region for plasma interaction in the inner divertor (point 10 in Fig 2.) is the final step towards deposition in the

louvre region. There is a thick repository of carbon at this point, which (it is believed) is supplied continuously by carbon transported from tiles 1 and 3. To what extent will deposition rates at the louvre region therefore reflect short-term changes in transport in the inner divertor? New QMBs are due to be installed at both inner and outer louvre regions. Further QMB experiments might thus address a number of questions:

(i) is a reduced rate of carbon supply from Tiles 1 and 3 (e.g. at lower divertor temperature) reflected in a reduced transport to the louvre region?
(ii) does the ablation rate remain similar, bit the size of the repository on Tile 4 (point 10) vary in magnitude?
(iii) what happens to the material that should be launched towards the outer louvres from the equivalent point on Tile 6 (point 16 in Fig.2)?
(iv) what rates will the QMBs measure if the magnetic field direction is reversed in JET?

The ^{13}C puffing experiment on the last day of the 2001 campaign confirmed that sources in the main chamber result in deposition at the inner divertor, and that there is no deposition at the outer divertor. All the discharges were identical L-mode pulses, and there were good Langmuir probe data from the divertor and from the reciprocating probe at the top of the vessel. Quantitative results on the deposition have also been presented earlier. Thus the data from the experiment provide a benchmark for plasma boundary modelling, which must explain whether the asymmetry in the deposition is due to flows in the SOL or some combination of plasma parameters in the outer divertor channel that makes deposition statistically improbable. A number of other parameter can be explored in further similar puffing experiments. These include:

(i) extension to H-mode discharges and different heating scenarios
(ii) measurement of the probability of impurities drifting to the inner divertor following injection at different poloidal positions
(iii) injection of impurities other than carbon

It is important to proceed with these valuable experiments for understanding SOL flow. Unfortunately each puffing experiment must be performed immediately prior to a vessel entry to retrieve samples, so only one experiment is possible per operational period.

The marker tiles fitted to main chamber limiters during 1999-2001 operations show areas of erosion at both the IWGL and OPL. Thus the tile analysis data provide evidence that much of the material deposited at the inner divertor was sputtered at the main chamber walls, ionised in and then transported along the SOL to the divertor without entering the plasma. However, generally on the marker stripes the erosion front is found to be within the Re interlayer. Sputtering away the Re requires energetic particles of >200eV, which may be multi-charged impurity ions or CXN. Erosion of carbon from uncoated areas of CFC may thus be much greater than the 2-3μm. In order to attempt a better quantitative balance between sources and sinks in JET, a larger coverage of “smart” tiles is planned, each of which can give a definitive value for the local carbon erosion.

CONCLUSIONS

The pattern of deposition in the JET Mk IIGB divertor was the same as in previous divertors: heavy deposition in the inner divertor channel and negligible net deposition in the outer channel. Carbon deposition (with high concentrations of trapped deuterium), occurred at shadowed areas at the inner divertor corner (as for the Mk IIA divertor). However, there was not a lot of deposition on the septum support structure (not present in Mk IIA), which may be significant for ITER. The source is principally in the main chamber, with material transported to the inner divertor along the SOL.

A fine demonstration of the SOL transport to the inner divertor was the ^{13}C tracer experiment performed on the last day prior to the shutdown at the end of the Mk IIGB phase, when $^{13}CH_4$ was injected during 13 identical pulses at the top of the JET vessel. High concentrations of ^{13}C were found at the surface of the inner divertor wall tiles ($^{13}C/^{12}C$ ~1), and a small amount at deposition sites at the inner limiters. No injected ^{13}C was resolvable outboard of the injection site. The experiment serves as a benchmark for modelling work.

Inner divertor wall tiles removed in 2001 were covered with a duplex film. The inner layer was very rich in metallic impurities, with Be/C ~1 and H-isotopes only present at low concentrations. The outer layer was about one-half the thickness of the inner layer, contained higher concentrations of D than normal for plasma-facing surfaces in JET (D/C ~0.4), and Be/C ~0.14. The origin of this outer layer is the subject of some speculation, but may result from the lower JET vessel (and divertor tile) temperatures for the last three months of the Mk IIGB campaign. The inner layer is similar in composition to that seen on Mk IIA inner divertor wall tiles, and also to Mk IIGB tiles removed prior to the change in temperature; the disparate outer layer does therefore not result from different behaviour for the two divertors. If the reduced transport during this period from the initial deposition site in the SOL to the shadowed areas is due to divertor temperature, then this also offers opportunities to ameliorate carbon transport (and hence tritium retention) in ITER.

ACKNOWLEDGEMENTS

This work has been conducted under the European Fusion Development Agreement and is partly funded by EURATOM, the UK Engineering and Physical Sciences Research Council, National Technology Agency of Finland and the Swedish Research Council.

REFERENCES

[1]. G. FEDERICI, et al., Nucl. Fusion **41** (2001) 1967.
[2]. J.P. COAD, B. FARMERY, Vacuum **45** (1994) 435.
[3]. D. WHYTE, J.P. COAD, P. FRANZEN, H. MAIER, Nucl. Fusion **39** (1999) 1025.
[4]. J.P. COAD, M. RUBEL, C.H. WU, J. Nucl. Mater. **241-243** (1997) 408.
[5]. M. RUBEL, et al., Phys. Scr., **T111** (2004), 112.
[6]. J.P. COAD, P. ANDREW, A.T. PEACOCK, Phys. Scr. **T81** (1999) 7.
[7]. J.P. COAD, et al., J. Nucl. Mater. **290-293** (2001) 224.
[8]. J.P. COAD, et al., J. Nucl. Mater. **313-316** (2003) 419.

[9]. D. STORK, (Ed.), Fusion Eng. Des. **47** (1999), *Special Issue: Technical Aspects of* Deuterium-Tritium Operation at JET.
[10]. C.H. SKINNER, et al., J. Nucl. Mater. **241-243** (1997) 214.
[11]. P. ANDREW, et al., Fusion Eng. Des. **47** (1999) 233.
[12]. R.D. PENZHORN, et al., J. Nucl. Mater. **288** (2001) 170.
[13]. N. BEKRIS, et al., J. Nucl. Mater., J. Nucl. Mater. **313-316** (2003) 501.
[14]. R.-D. PENZHORN, et al., Fusion Eng. Des. **49-50** (2000) 753.
[15]. M. RUBEL, et al. J. Nucl. Mater. **313-316** (2003) 323.
[16]. A.C. ROLFE, Fusion Eng. Des. **36** (1997) 91.
[17]. R.A. PITTS, et al., J. Nucl. Mater. **313-316** (2003) 777.
[18]. J. LIKONEN, et al., Fusion Eng. Des. **66-68** (2003) 219.
[19]. J.P. SCHIFFER, et al., Nucl. Phys. **15** (1956) 1064.
[20]. E.A. MILNE, Phys. Rev. **93** (1954) 762.
[21]. M. RUBEL, P. WIENHOLD, D. HILDEBRANDT, Vacuum **70** (2003) 423.
[22]. G.F. MATTHEWS, et al, 28th EPS Conf. on Controlled Fusion and Plasma Physics, Funchal (2000), ECA **25A** 1613
[23]. M. MAYER, SIMNRA User's Guide, Report IPP 9/113, Max-Planck-Institut für Plasmaphysik, Garching, Germany, 1997.
[24]. S.J. SNIPE, et al, Proc. of 21st Symposium on Fusion Technology (SOFT21), September 2000
[25]. E. GAUTHIER, et al., *"Thermal behaviour of re-deposited layer under high heat flux exposure"*, 16th Int. Conf. on Plasma-Surface Interactions in Controlled Fusion Devices, Portland, Maine, USA, May 2004.
[26]. T. TANABE, et al., J. Nucl. Mater. **313-316** (2003) 478.
[27]. J.P. COAD, et al, 26th EPS Conf. on Controlled Fusion and Plasma Physics, Maastricht, June 1999
[28]. M. MAYER, R. BEHRISCH, P. ANDREW, J.P. COAD, A.T. PEACOCK, et al., Phys. Scr. **T81** (1999) 13.
[29]. H.G. ESSER, et al., Phys. Scr. **T111** (2004) 129.
[30]. M. RUBEL, V. PHILIPPS, A. HUBER, and T. TANABE, Physica Scripta **T81** (1999) 61
[31]. R. NEU, et al, J Nucl. Materials **290-293** (2001) 206
[32]. G.F. MATTHEWS, et al., Proc. 30th EPS Conf. on Plasma Physics and Controlled Fusion, ECA Vol. **27A,** P-3.198, St. Petersburg, Russia, July 2003.
[33]. M. MAYER, et al., Proc. 30th EPS Conf. on Plasma Physics and Controlled Fusion, ECA Vol. **27A,** O-2.6A**,** St. Petersburg, Russia, July 2003.
[34]. H.G. ESSER, et al., *"Effect of plasma configuration and reversed grad B on carbon migration measured in the inner divertor of JET"*, Proc. 16th Int. Conf. on Plasma-Surface Interactions in Controlled Fusion Devices, Portland, Maine, USA, May 2004.
[35]. P.A. ANDREW, et al., "Outer divertor target impurity deposition during reversed field *operation in JET"*, Proc. 16th Int. Conf. on Plasma-Surface Interactions in Controlled Fusion Devices, Portland, Maine, USA, May 2004.

[36]. J. LIKONEN, et al., *"Beryllium accumulation at the inner divertor of JET"*, Proc. of 16th Intern. Conf. on Plasma Surface Interactions in Controlled Fusion Devices, Portland, Maine, USA, May 2004.

[37]. M. MEIER, A. VON KEUDELL, and W. JACOB, Nuclear Fusion **43** (2003) 25-2

Probe	Ion flux ($10^{26}m^{-2}$) 1998–1999	Ion flux ($10^{26}m^{-2}$) 1999–2001	Ion flux ($10^{26}m^{-2}$) 1998–2001
1	0.00	0.00	0.00
2	0.086	0.840	0.926
3	0.142	0.799	0.941
4	0.090	0.650	0.740
5	0.959	2.98	3.94
6	4.25	4.39	8.64
7	4.96	3.69	8.65
8	4.55	5.78	1.03
9	1.95	1.14	3.09

JG05.13-1c

Table 1:
Cumulative ion fluxes measured with Langmuir probes for experimental campaigns 1998-1999, 1999-2001 and 1998-2001.

Element/ Isotope	Reaction/Method	Energy (MeV)	Sensitivity (atoms cm^{-2})	Remarks
D	$^{3}He(d,p)^{4}He$/NRA	0.7– 3	1×10^{14}	Depth profiling Very high selectivity
Be– 9	$^{3}He(^{9}Be,p)^{11}B$/NRA	2.5	1×10^{17}	Not well defined cross–section
B– 11	$p(^{11}B,a)^{8}Be$/NRA	0.7	4×10^{14}	No depth profiling
C– 12	$^{3}He(^{12}C,p)^{14}N$/NRA $p(^{12}C,^{12}C)p$/EPS	2.5 1.5	1×10^{17} 3×10^{16}	
C– 13	$^{3}He(^{13}C,p)^{15}N$/NRA $p(^{13}C,^{13}C)p$/EPS $p(^{13}C,^{13}C)p$/EPS	2.5 2.5 1.442 (resonance)	1×10^{17} 3×10^{16} 5×10^{15}	Quantitative for layers <50nm
i, Cr, Fe	H^{+}/PIXE	2.5		
Re	^{4}He+/RBS H^{+}/PIXE	2.5 2.5	3×10^{12}	

JG05.13-2c

Table 2:
Characteristic parameters for accelerator-based ion beam analysis.

Layer	D,at.%	Be,at.%	^{12}C,at.%	^{13}C,at.%	O	Thickness (10^{15} atoms/cm^2)
1	11	5	27	31	26	2686
2	30	5	53	0	10	20839
3	5	30	33	0	28	20483

JG05.13-3c

Table 3:
Results of SIMNRA simulations of an RBS spectrum (shown in Fig. 12) recorded from near the bottom of Tile 1 from Set B (exposed 1999-2001).

Tile set/ exposure period	A / 1998–1999	C / 1998–2001	B / 1999–2001
Location: Octant in JET	4D	5C	4D
^{13}C layer	Not exposed to $^{13}CH_4$	Surface layer	Surface layer
C–D layer	No outer C–, D– rich layer	Outer C–, D– rich layer*	Outer C–, D– rich layer
Be layer	Outer be-rich layer*	Inner be-rich layer*	Inner be-rich layer
Film thickness (μm)	~1.3 μm**	Total ~ 6.8 μm**	Total ~ 5.2 μm**

JG05.13-4c

* but amounts ~50% greater for tiles exposed 1998-2001 than exposed 1999-2001

** based on 10^{19} atoms cm^{-2} equivalent to 1.25μm

Table 4:
Summary of analysis results for the equivalent poloidal position at the bottom of inner divertor Tiles 1 exposed to different periods

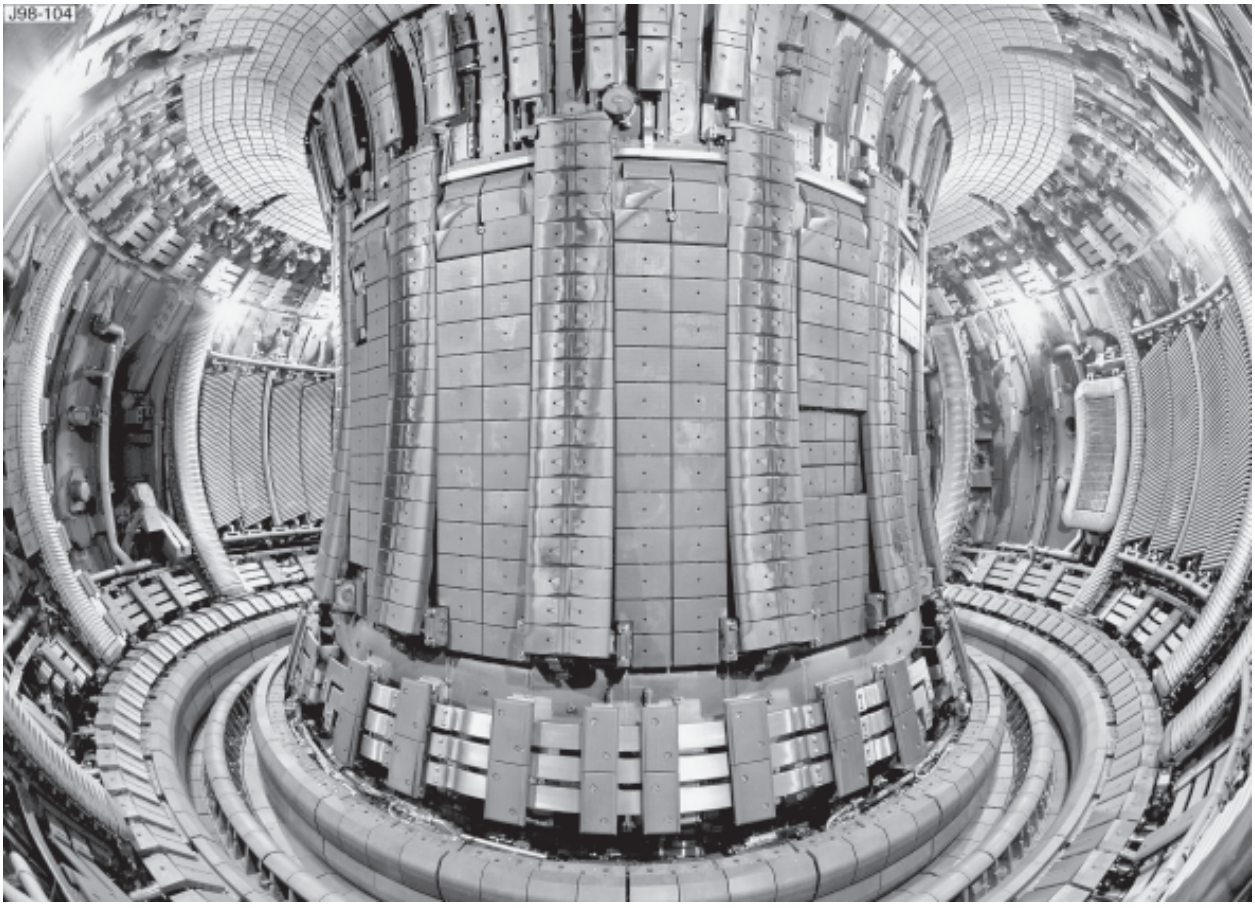

Figure 1: JET vacuum vessel with the Gas Box divertor.

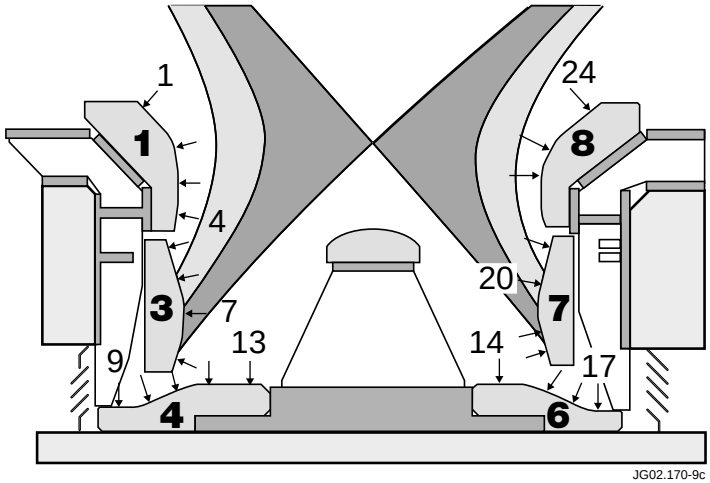

Figure 2(a): Poloidal cross-section of the Mk-IIGB divertor, the flux deposition profiles and distribution of mechanical measurement points.

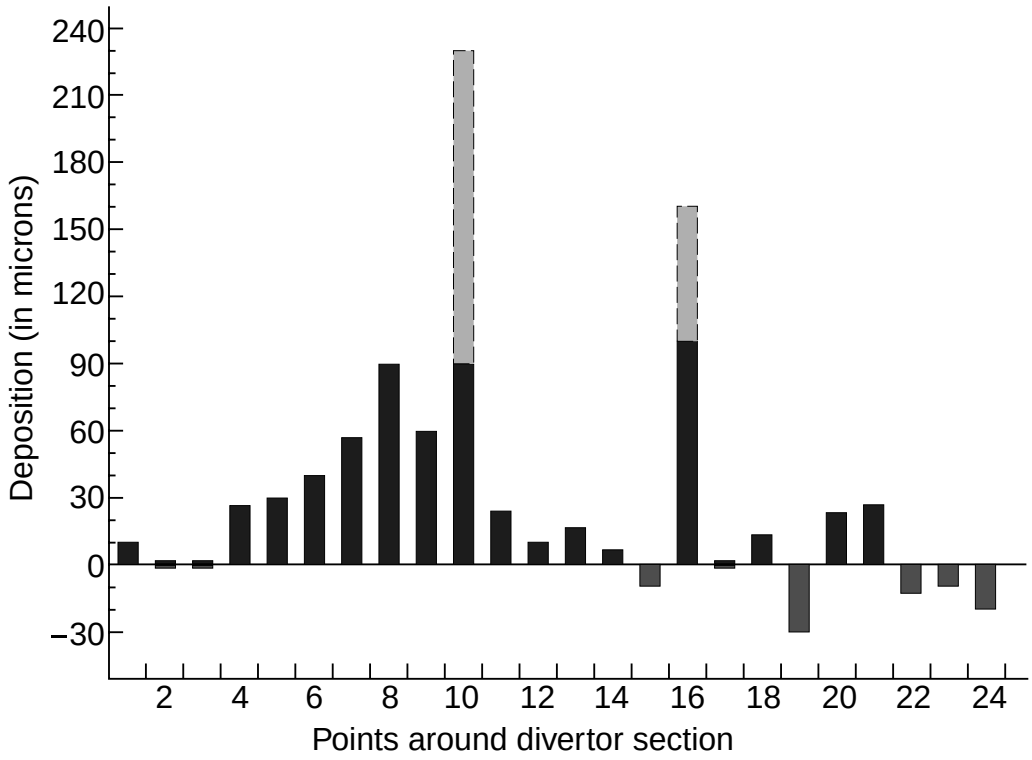

Figure 2(b):Time line showing the Mk IIGB operational history, and the exposure periods of samples

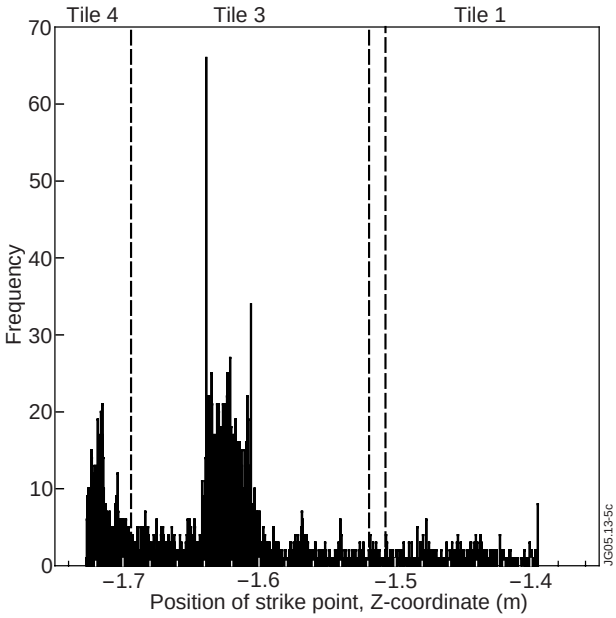

Figure 3: Histogram of the inner strike point positions (Z-coordinate). Position of inner divertor Tiles 1 and 3 is indicated with vertical dashed lines.

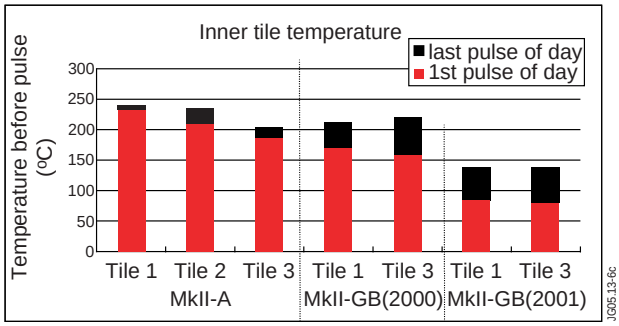

Figure 4: Histogram of tile temperatures in the inner target during operation with the Mk-IIA and Gas Box (in 2000 and 2001) divertors.

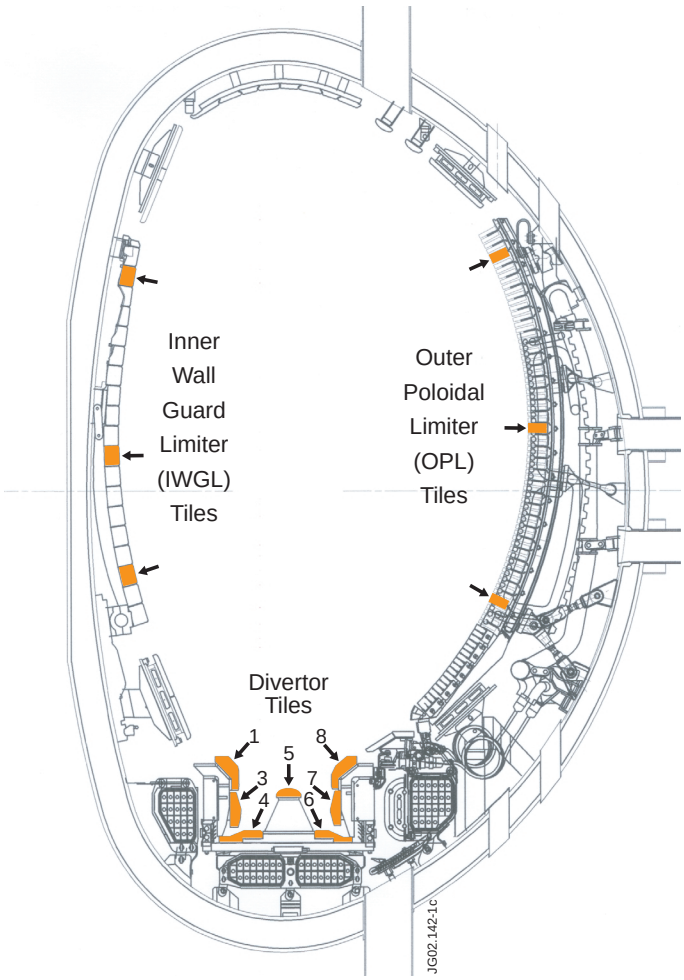

Figure 5: Location of marker tiles on the main chamber wall and in the divertor.

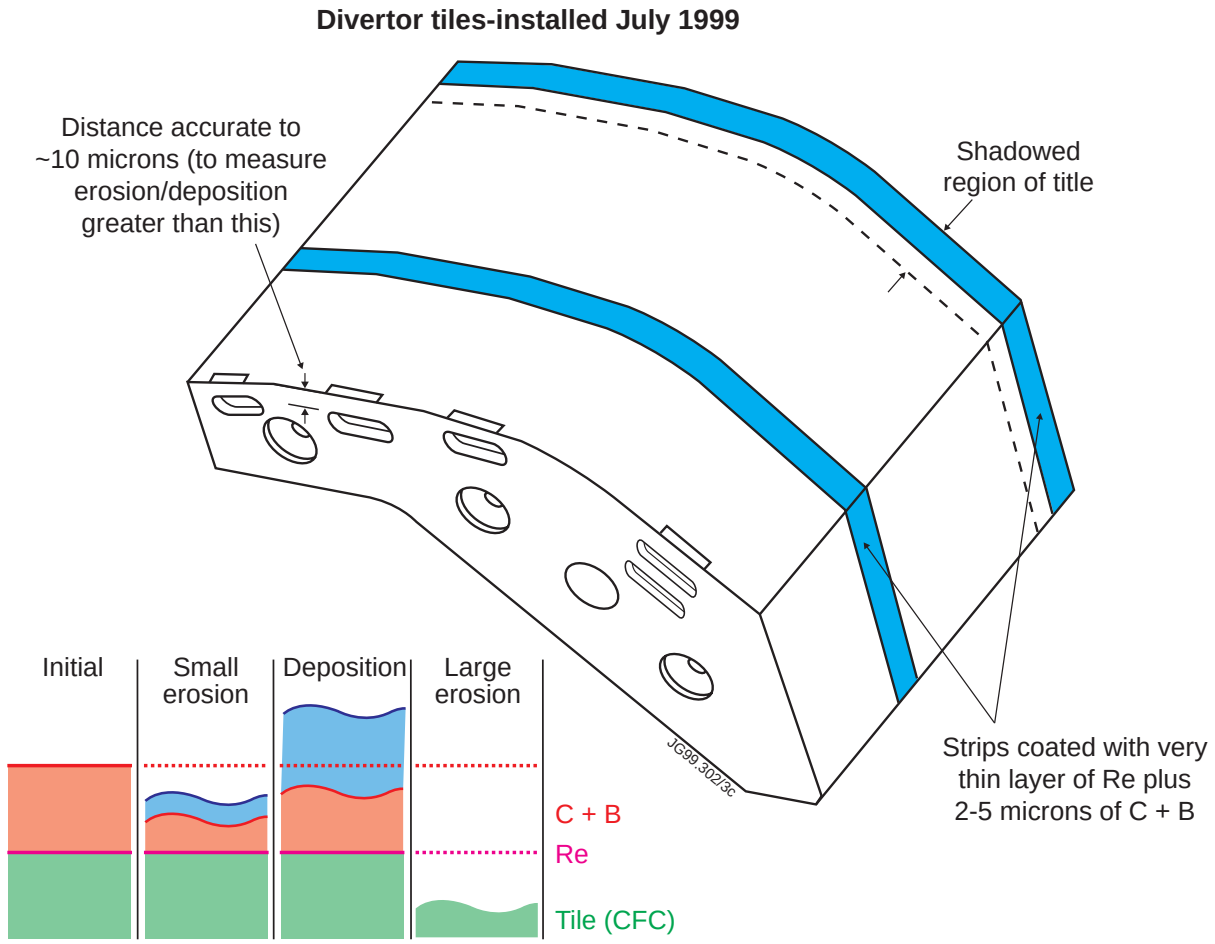

Figure 6: Schematic view of a marker tile and the desription of the idea for using such tiles in erosion and deposition studies.

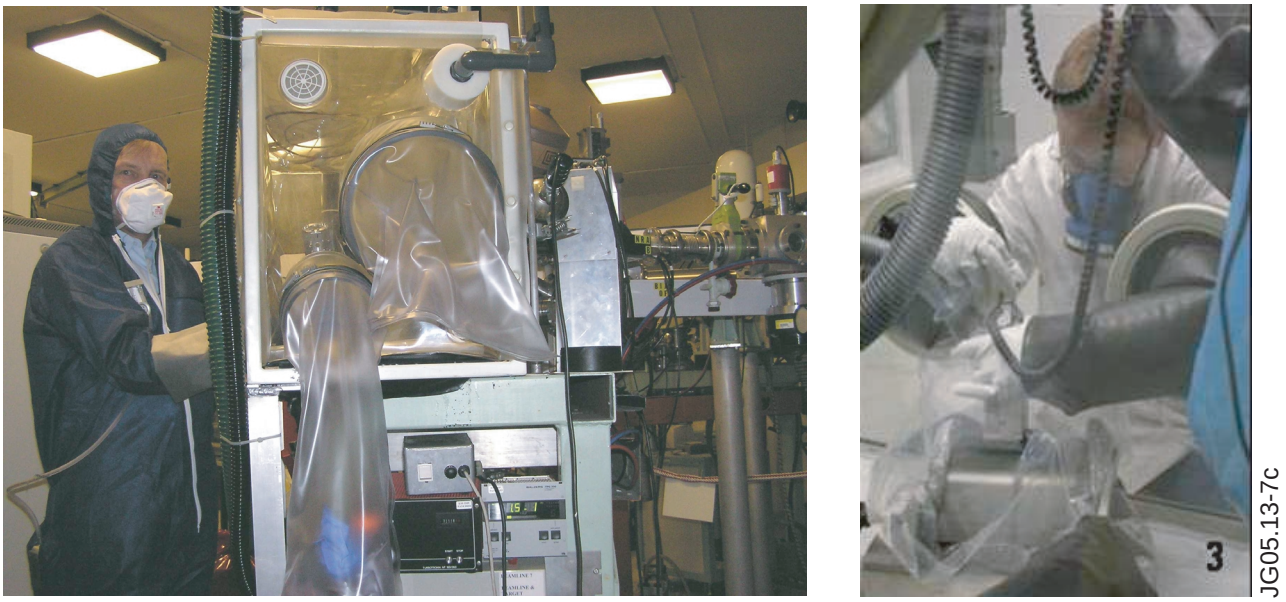

Figure 7: Handling facilities for beryllium and tritium contaminated materials in surface analysis laboratories: (a) loading samples to the analysis chamber in the accelerator laboratory at the University of Sussex; (b coring of samples in the SIMS laboratory at VTT.

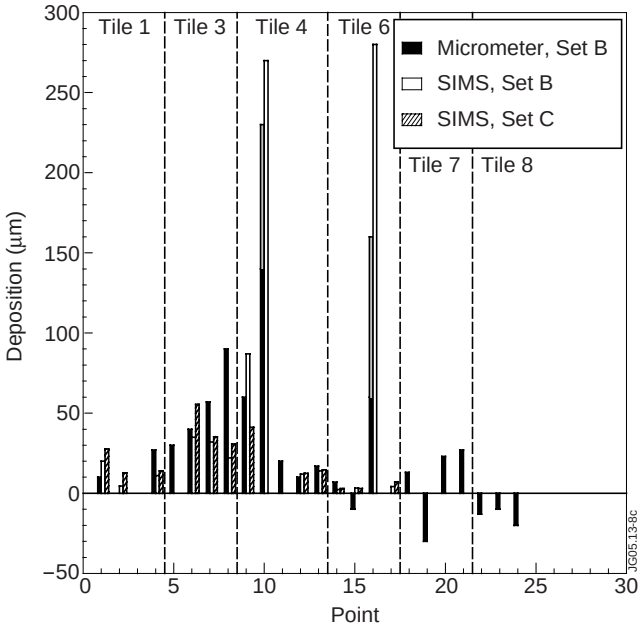

Figure 8: Surface measurements with a micrometer and SIMS on the poloidal set of divertor tiles, the change of the surface layer thickness.

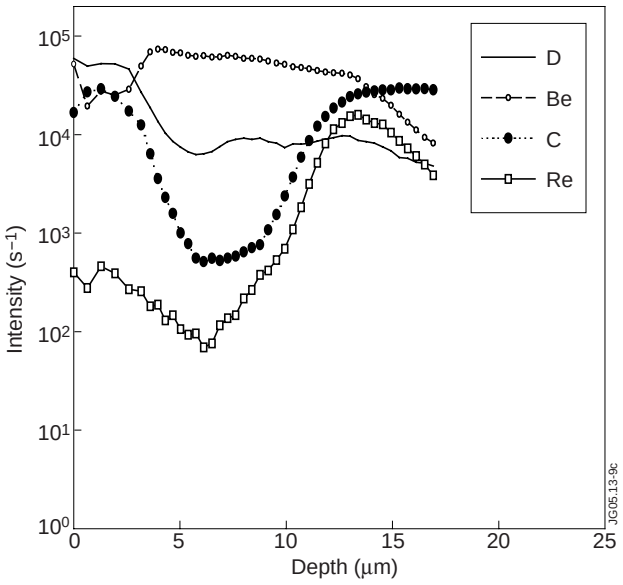

Figure 9: SIMS depth profile of deuterium, beryllium, carbon and rhenium on the bottom of Tile 1 (point 4 in Fig. 2) exposed in the period 1999-2001 (Set B).

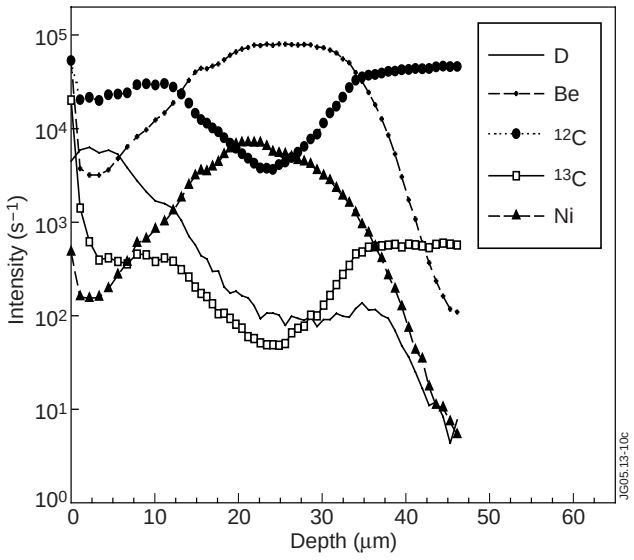

Figure 10: SIMS depth profile of deuterium, beryllium, carbon and nickel in the central part of Tile 3 (point 7 in Fig. 2) exposed in the period 1999-2001 (Set B

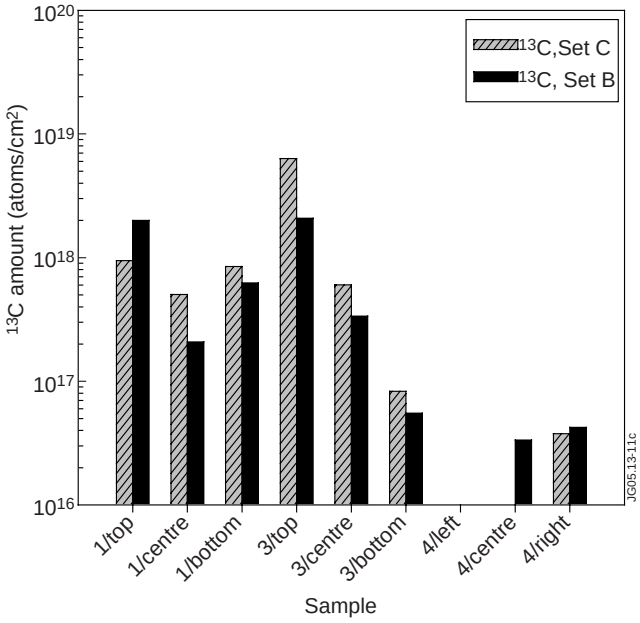

Figure 11: ^{13}C amounts found on the divertor Tile 1, 3 and 4 of Set B and C. Analysed samples from from top, centre and bottom of Tiles 1 and 3. Samples from Tile 4 were from an area shadowed by the louvers (4/left), from centre and from an area shadowed by the septum (4/right).

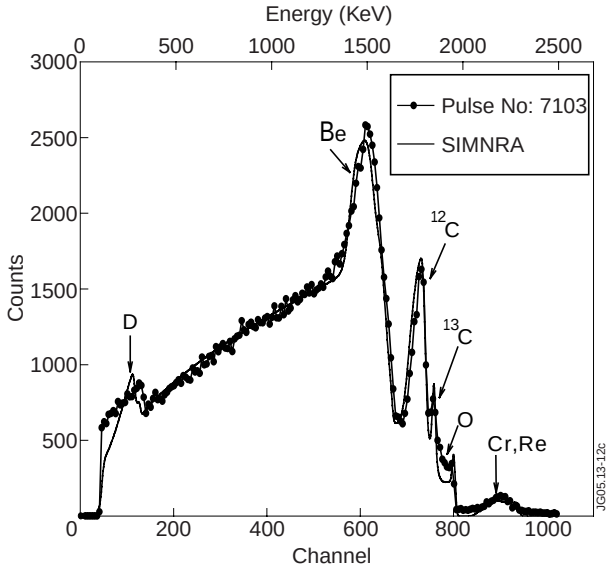

Figure 12: Experimental and SIMNRA simulated Rutherford backscattering spectra from the bottom of Tile 1 exposed in 1999-2001 (Set B).

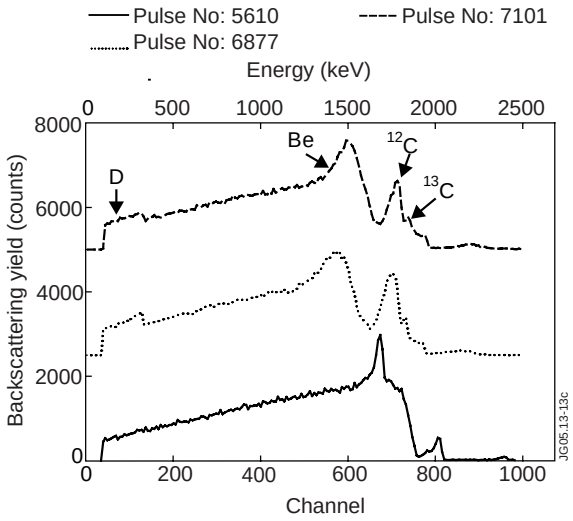

Figure 13: Comparison of RBS spectra from similar points (towards the bottom of the front face of Tile 1) on Set A (JET 5610), Set B (JET 7103) and Set C (JET 6877).

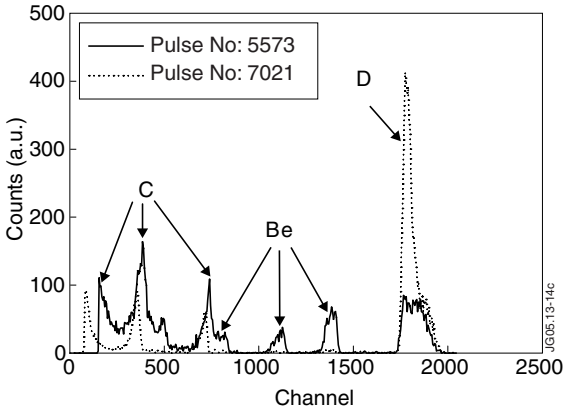

Figure 14: Comparison of NRA from the centre of Tile 3 of Set A (JET 5573) and Set B (JET 7021).

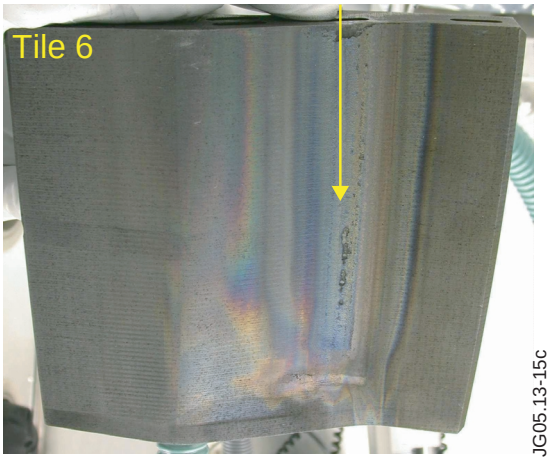

Figure 15: Appearance of the exposed Tile 6. Friable band on the sloping region is indicated by the arrow.

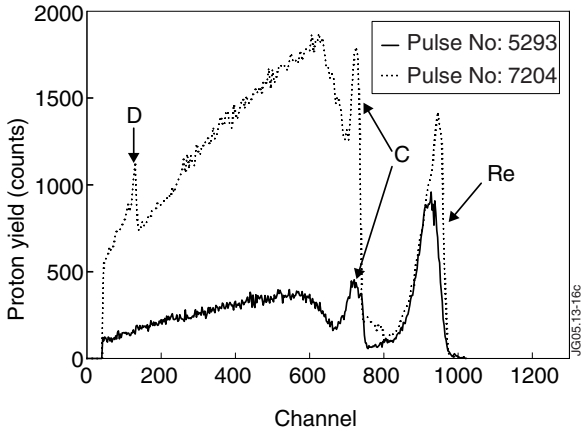

Figure 16: RBS spectrum for Tile 6 (near point 14 in Fig. 2) of Set B ***(JET 7204) and*** *from coated tile before exposure (JET 5293).*

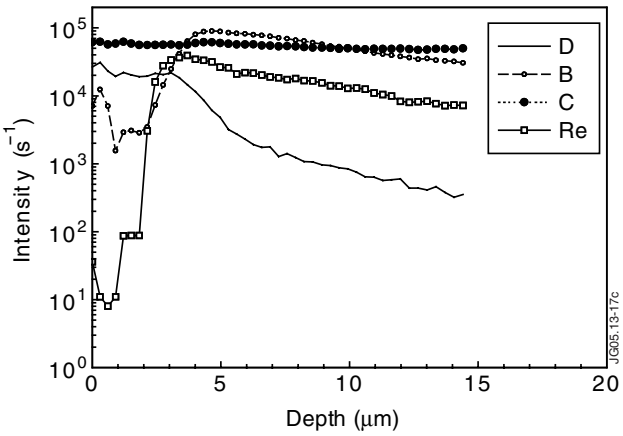

Figure 17: SIMS depth profiles from near point 14 (see Fig. 2), removed from divertor base Tile G6C after exposure in JET 1999-2001.

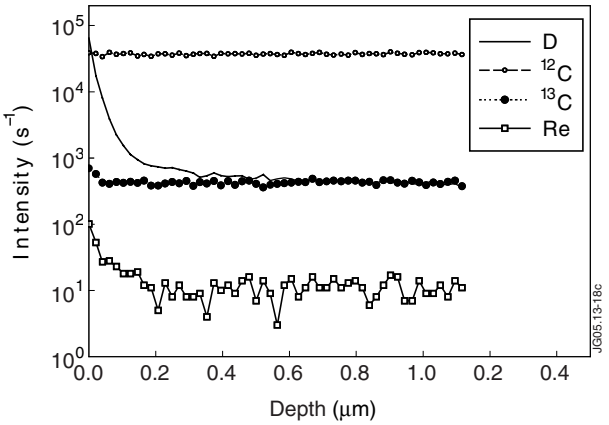

Figure 18: SIMS depth profile of deuterium, carbon (12 and 13) and rhenium from the centre of Tile 7 exposed in the period 1999-2001 (Set B).

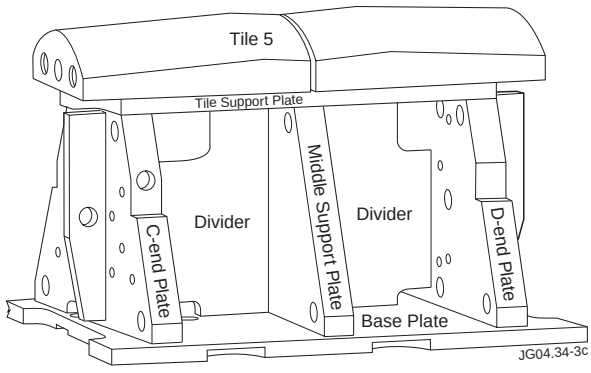

Figure 19: Structure of the Gas Box module.

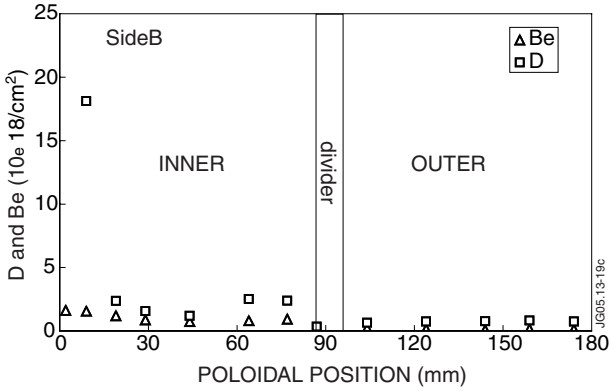

Figure 20: Poloidal distribution of deuterium and beryllium on the middle support plate of the gas box.

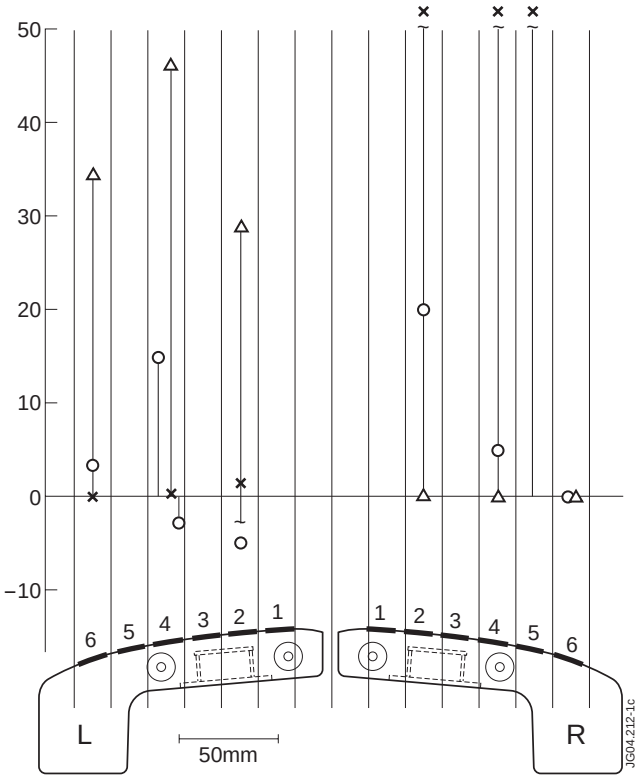

Figure 21: Cross-section of a pair of IWGL tiles and a plot of the amount of erosion/deposition at each sample analysed by SIMS. Crosses: tiles 2X2R/L, circles: 3X11R/L, triangles: 3X17R/L

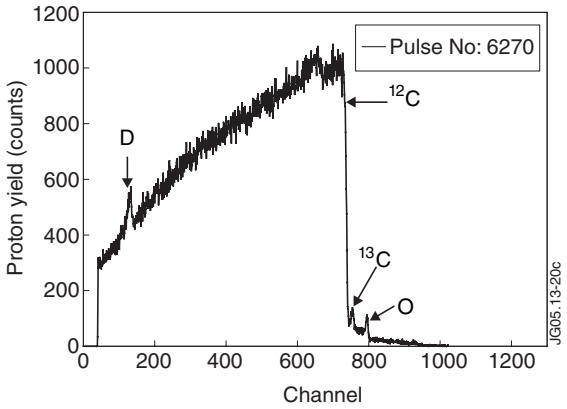

Figure 22: RBS spectrum (JET6270) from near the centre of IWGL tile 2X2R (Set B).

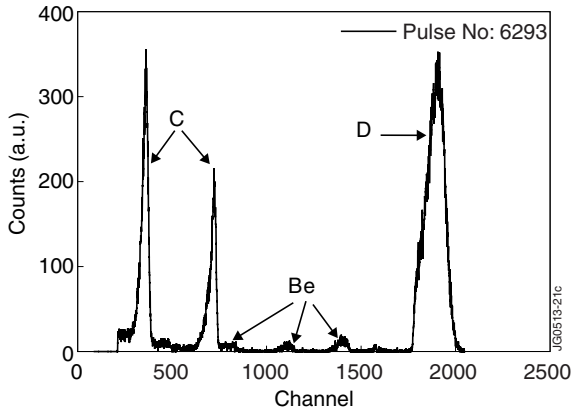

Figure 23: NRA spectrum from near the centre of Tile 2X2R (Set B).

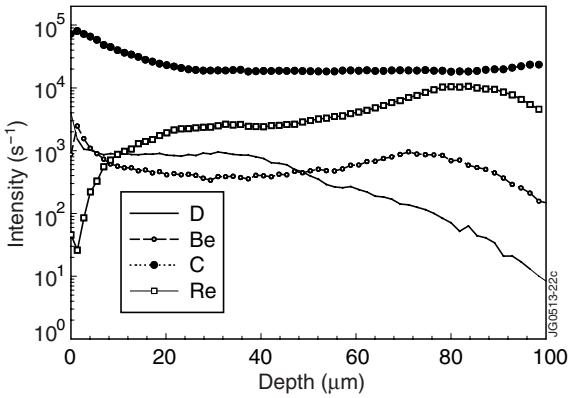

Figure 24: SIMS depth profile of deuterium, beryllium, carbon and rhenium near the centre of Tile 2X2R exposed in the period 1999-2001 (Set B).

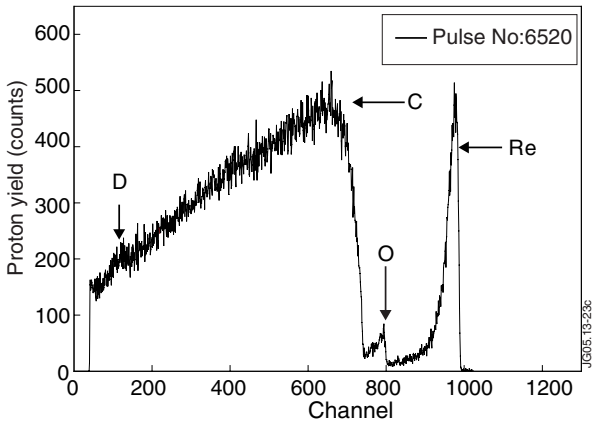

Figure 25: RBS spectrum (JET 6270) from the tangency point of IWGL Tile 3X17R (Set B).

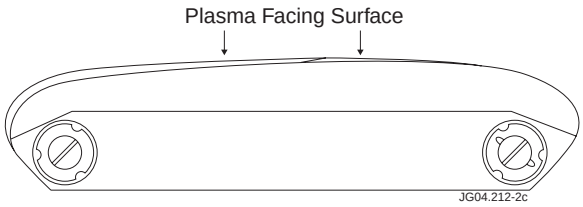

Figure 26: Cross-section of an outer poloidal limiter tile

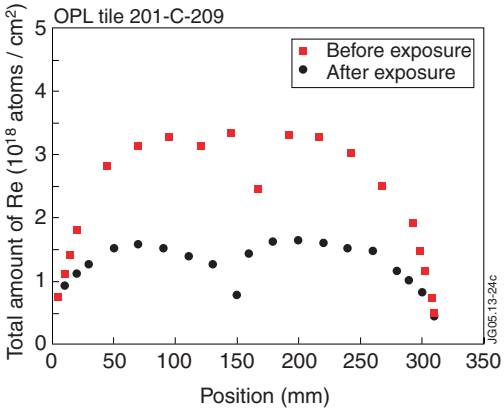

Figure 27: Amounts of Re measured by RBS and calculated using SIMNRA on OPL tile 8B21 before and after exposure in JET 1999-2001.

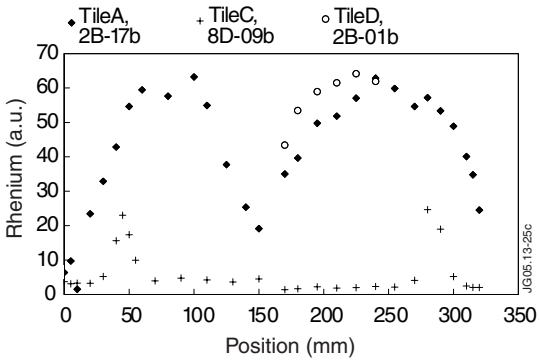

Figure 28: Rhenium signals from three tiles of the outer poloidal limiters (OPL). Tiles A, C and D are from the bottom, centre and top of the OPL, respectively. Peak Re signals in the central region prior to exposure were ~160 (a.u.).

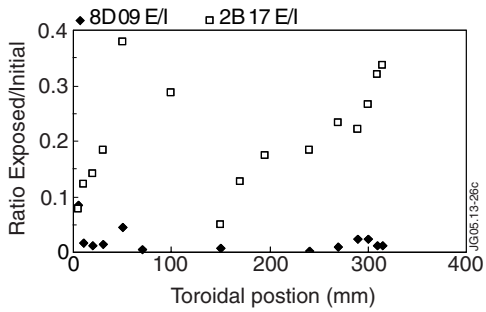

Figure 29: Ratio of boron detected after exposure in JET to that measured before exposure for tiles 2B 17 and 8D 09.

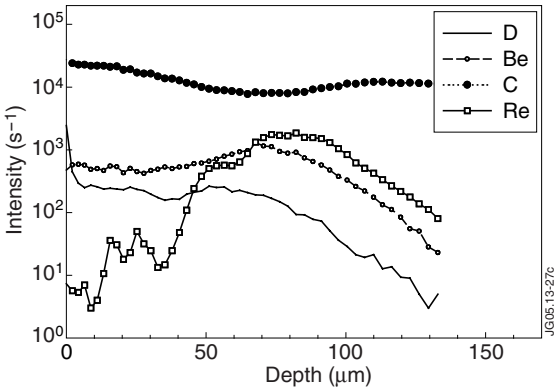

Figure 30: SIMS depth profile from the end of tile 8D09.